TIME COURSE OF SIGNALING PROCESSES INVOLVED WITH EXTRACELLULAR OSMOTIC-INDUCED GLUCOSE UPTAKE IN MAMMALIAN SKELETAL MUSCLE

Adrian J. Lui, BSc. Kin. (Honours)

Submitted in partial fulfillment of the requirements for the degree of
Master of Science in Applied Health Sciences
(Kinesiology)

Supervisor: Brian Roy, PhD

Faculty of Applied Health Sciences, Brock University
St. Catharines, Ontario

Abstract

TIME COURSE OF SIGNALING PROCESSES INVOLVED WITH EXTRACELLULAR OSMOTIC-INDUCED GLUCOSE UPTAKE IN MAMMALIAN SKELETAL MUSCLE

Adrian Lui
Brock University

Advisor:
Dr. Brian Roy

Extracellular hyper-osmotic (HYPER) stress increases glucose uptake to defend cell volume, when compared to iso-osmotic (ISO) conditions in skeletal muscle. The purpose of this study was to determine a time course for changes in common signaling proteins involved in glucose uptake during acute hyper-osmotic stress in isolated mammalian skeletal muscle. Rat extensor digitorum longus (EDL) muscles were excised and incubated in a media formulated to mimic ISO (290 ± 10 mmol/kg) or HYPER (400 ± 10 mmol/kg) extracellular condition (Sigma Media-199). Signaling mechanisms were investigated by determining the phosphorylation states of Akt, AMPK, AS160, cPKC and ERK after 30, 45 and 60 minutes of incubation. AS160 was found to be significantly more phosphorylated in HYPER conditions compared to ISO after 30 minutes ($p<0.01$). It is speculated that AS160 phosphorylation may facilitate an increase in glucose uptake under hyper-osmotic stress, possibly by initiating cellular signalling to increase glucose transporter 4 (GLUT4) content at the cell surface.

Acknowledgements

First and foremost, I would like to thank my supervisor Dr. Brian Roy for accepting me as his student. I have learned much more than just physiology and metabolism during my time at Brock University. I've learned the value of hard work, dedication and perseverance, and for that I am grateful. Thank you to Dr. Sandra Peters and Dr. Paul LeBlanc for providing always having an open door with sound advice. Last but not least, thank you to all my lab mates whom I'm experienced the ups and downs of academia with. Good luck to all in future endeavours.

Table of Contents

List of Figures

List of Tables

List of Abbreviations

ADP – Adenosine Diphosphate

aPKC – atypical Protein Kinase C

cPKC – conventional Protein Kinase C

AICAR – 5-aminoimidazole-4-carboxamide-riboside

AMP – Adenosine Monophosphate

AMPK – AMP Activated Protein Kinase

AS160 – Akt Substrate of 160 kDa

ATP – Adenosine Triphosphate

CaMK – Calmodulin Kinase

CaMKK – Calmodulin Kinase Kinase

CAP - c-Cbl Associated Protein

CBD – Calmodulin-Binding Domain

cGMP – Cyclic Guanosine Monophosphate

DHPR – Dihydropyridine Receptors

DNP – Dinitrophenol

ECF – Extracellular Fluid

EDL – Extensor Digitorum Longus

ERK – Extracellular Related Kinase

ETC – Electron Transport Chain

FAD^+ - Flavin Adenine Dincleotide

$FADH_2$ - Flavin Adenine Dincleotide (Reduced Form)

G-1-P – Glucose-1-phosphate

G-6-P – Glucose-6-phosphate

G-6-Pase – Glucose-6-phosphatase

GLUT – Glucose Transporter

GP – Glycogen Phosphorylase

GPK – Glycogen Phosphorlyase Kinase

GS – Glycogen Synthase

GSK – Glycogen Synthase Kinase

GTP - Guanosine Triphosphate

HK – Hexokinase

HYPER – Hyper-osmotic

HYPO – Hypo-osmotic

ICF – Intracellular Fluid

IR – Insulin Receptor

IRS – Insulin Receptor Substrate

ISO – Iso-Osmotic

Kg – Kilogram

KO – Knockout

MAPK – Mitogen Activated Protein Kinase

mM – millimolar

mmol/kg – millimoles per kilogram

mOsm – milli-osmoles

NaCl – Sodium Chloride

NAD^+ – Nicinamide Adenine Dinucleotide

NADH - Nicinamide Adenine Dinucleotide (Reduced Form)

NKCC – Na^+ -K^+ -2Cl^- co-transporters

NO – Nitric Oxide

NOS – Nitric Oxide Synthase

NSF - Nitrogen-ethylmaleimide-sensitive factor

PCr – Phosphate Creatine

PKB – Protein Kinase B

PKC – Protein Kinase C

PDH – Pyruvate Dehydrogenase

PDK – Phosphatidylinositol- Dependant Kinase

PI3-K – Phosphatidyl Inostiol 3-Kinase

PIP_2 – Phosphatidyl Inostiol Diphosphate

PIP_3 - Phosphatidyl Inostiol Triphosphate

PLD – Phopholipase D

PP1 – Phosphoprotein Phosphatase

PYK – Proline-Rich Kinase

RVD – Regulatory Volume Decrease

RVI – Regulatory Volume Increase

RyR – Ryanodine Receptors

Ser - Serine

SH2 – Src Homology

SiRNA – Silencing Ribonuclieic Aside

SNARE – Soluble NSF Attachment Protein

v-SNARE – vesicle SNARE

t-SNARE – target SNARE

SR – Sarcoplasmic Reticulum

TBW – Total Body Water

TeTx – Tetanus Toxin

TGN – Trans-Golgi Network

Thr – Threonine

T-Tubules – Transverse Tubules

VAMP – vesicle associated membrane protein

1. Water – The Universal Solvent

1.1 Introduction

Water is the quintessential nutrient of life. The human body is a well refined machine that has the remarkable ability to regulate its water levels in very precise quantities. When the human body is placed under various internal and external stresses, it has the capacity to acutely alter its functional capacity to counteract disturbances that threaten homeostasis [69]. In 1994, Dieter Häussinger introduced the "Cell Swelling Theory". This concept suggested that cell volume is a key regulator of cellular metabolism where cell swelling induces a state of cell anabolism, and cell shrinking induces a state of cell catabolism [62]. This theory attempts to explain the body's ability to counteract disturbances (cell volume change) to maintain homeostasis.

In spite of tightly regulated whole body hydration status, dehydration can occur and alter cardiovascular, thermoregulatory, central nervous system and metabolic functions in humans [70]. During exercise and increased physical efforts, sweat output often exceeds water intake, resulting in total body water deficiency (hypohydration) [70]. A modest 2% decline in body weight due to dehydration can result in mild dysfunction in any of the aforementioned systems [79]. Hypohydration can also result in severe ramifications for exercise performance and prolong periods of dehydration can prove to be fatal within several days or sooner [62].

Total body water (TBW) varies from person to person. Many factors such as body composition, age and physical activity level can influence an individual's TBW. An average, 70kg person is said to be carrying ~60% of their weight as water. In absolute terms, this would equate to ~42 kg or 42 litres of TBW [61]. Seventy-three percent of TBW is found in the lean body mass (skeletal muscle, bone, organs) while only 10% is found in the fat mass; therefore,

total body water is largely dependent on lean body mass. [69]. Skeletal muscle accounts for 40-50% of total body mass and therefore it is considered one of the most important tissues in regards to fluid homeostasis in the human body [58].

1.2 Water Compartments

Muscle cells are not in direct contact with the "outside world". Instead, extracellular fluid (EFC) surrounds a cell's membrane and acts as a medium for communication with other cells. The ECF is categorized into two different compartments which are physically separated by the vessel walls of the circulatory system. Plasma, the fluid portion of blood, lies within the blood vessels and is considered one compartment. The other portion, known as interstitial fluid, lies outside the circulatory system and outside cells. Not only is interstitial fluid a medium for cell to cell communication, it also functions as a nutrient source and waste disposal site for cells. The vast amount of fluid exchange between the vasculature and tissue occurs at the level of the capillaries; where both the vessel walls and the endothelium are thin, minimizing the diffusion distance between the two compartments.

Fluid exchange is a regulated process between the ECF (~1/3 of total body water) and the intracellular fluid (ICF; ~2/3 of total body water). While ICF is primarily comprised of water, it contains numerous molecules required for normal cell function including ions and amino acids. Cellular organelles, such as the mitochondria, are suspended within the ICF and interact with the ICF to regulate ion concentration inside and outside each organelle. Maintaining proper water balance (and subsequently ion concentration) between the ICF and organelles is crucial for optimal function and even cell survival.

Osmosis is the fundamental concept that governs the movement of water between compartments. It is defined as passive fluid (water) movement through a semi-permeable

membrane in response to a solute concentration gradient [40]. Fluid movement between compartments is highly selective. Compartment barriers (cell membranes and capillary endothelium) are not only responsive to ion concentration, but the type of ion as well. There are four mechanisms that determine water distribution in various compartments: hydrostatic pressure, crystalloid pressure, ion pumps and colloidal pressure [40]. Hydrostatic pressure represents the pressure of fluids exerted against membranes or vessel walls. Elevations in hydrostatic pressure force fluids and solutes across membranes (e.g. from the capillaries to the interstitial space). Crystalloid pressure is the pressure exerted from within a fluid due to dissolved mineral salts (ie. Na^+ and Cl^-) and other water-soluble molecules. These solutes generally move more freely across membranes to influence osmotic pressure, however, mammalian cells lack a firm cell wall, therefore generating negligibly low hydrostatic and crystalloid pressure [42, 53]. Colloid osmotic pressure is defined as the pressure exerted on membranes by large non-permeable solutes [40]. Colloids do not move as freely across cell membranes, and as such the cells reach osmotic equilibrium through the movement of water to compensate for accumulation or loss of these molecules. Skeletal muscle cells primarily use ion pumps to actively transport ions against concentration gradients. This concept is extremely important when regulating cell volume and is explained below. Water moves from an area of low solute concentration to an area of high solute concentration. Thus, the amount of water movement is dependent on the osmolality of the solution.

Molarity is used to describe the concentration of a solute in a solution and is measured using the unit *mole/litre* (mol/L). Consequently, molarity represents the number of molecules (6.02×10^{23} molecules/mole) in the solution. However, *osmolarity* is a more useful unit of measurement to predict osmosis and it describes the number of particles (not molecules) per litre of solution (Osmol/L). Particles include dissociated ions and fully intact molecules,

regardless of molecular size and weight. For example, when a single NaCl molecule is placed in a solution, it will dissociate into Na^+ and Cl^- ions. The solution would then contain more particles than a solution with just one glucose particle. Two solutions with an equal number of particles are considered iso-osmotic. A solution is hyper-osmotic if it has more particles relative to another solution. Likewise, a solution is hypo-osmotic if it contains fewer particles relative to another. Lastly, in highly concentrated solutions, particles can significantly influence the weight of a solution. Therefore, *osmolality* is a term expressed in osmoles per kilogram of water. However in biological solutions, solutes (usually measured in milliosmoles) contribute very little to the overall weight of the solution, so osmolarity and osmolality may sometimes be interchanged. Nevertheless, neither osmolarity nor osmolality can accurately determine water movement between compartments, and as such tonicity must also be known [72].

Tonicity is simply described as the osmotic pressure or tension of a solution. When a cell is placed in a hypertonic solution, it shrinks, as fluid is drawn out of the cell. The opposite is true when a cell is placed in a hypotonic solution, it swells. Lastly, if a cell does not change size, the solution is termed isotonic. Tonicity has no units and is only a comparative term. The distinction between osmolarity and tonicity lies in the permeability characteristics of the solutes. Tonicity accounts only for water movement, dictated by non-penetrating solutes, while osmolarity is dictated by both penetrating and non-penetrating solutes. Solutions containing non-penetrating solutes can only equalize an osmotic gradient through the movement of water. However, solutions with penetrating solutes can neutralize concentration gradients through movement of both solutes and water. Therefore, it is possible for a solution to be hyper-osmotic yet isotonic; where penetrating solutes migrate out of the cell into the extracellular space therefore equilibrating the osmotic gradient without the net movement of water [72].

1.3 Cell Volume Regulation

Cells react to volume perturbations by activating volume regulatory mechanisms to manipulate osmolality and consequently water movement. Osmolality manipulates cell volume through the uptake and release of inorganic ions and small organic osmolytes [75]. Ion movement is responsible for two-thirds of cell volume regulation while the release and uptake of organic osmolytes (such as glucose) is responsible for the other third [43]. Regulatory volume increase (RVI) is a mechanism activated to acutely counteract cell shrinkage, usually initiated in hyper-osmotic and hypertonic extracellular environments. The time course of RVI is dependent on many factors such as cell type, however, RVI stimulated by inorganic ions typically occurs over a period of minutes [75]. RVI stimulated through the uptake of organic osmolytes is a slower process that can take hours [75]. RVI is primarily accomplished as a result of ion movement through the Na^+ -K^+ -2Cl^- co-transporters (NKCC) in combination with the Na^+/H^+ exchangers and Cl^-/HCO_3^- exchangers. The NKCC results an inward flux of Na^+, K^+ and Cl^-. The net effect of the two exchangers results in the uptake of NaCl which increase intracellular osmolality and promotes an influx of water into the cell [42]. Throughout RVI, the Na^+/K^+ ATPase continues to expel Na^+ thus resulting in a net uptake of K^+ and Cl^-. The Cl^- ion follows K^+ through the cell membrane to maintain an electrical potential. RVI is a process that requires additional energy due to the increase in flux through the Na^+/K^+ ATPase. Recall that RVI is also accomplished through the net uptake of organic osmolytes such as glucose [75]. The uptake of glucose serves two useful purposes. First, glucose uptake will increase intracellular osmolality; secondly, it can also be used as a substrate for glycolysis for increased energy production. In addition, the uptake of osmolytes reduces the destabilizing effects caused by inorganic ions and/or cellular proteins [42]. Therefore the uptake of glucose and other osmolytes is more favourable than the uptake of inorganic ions. Regulatory volume decrease (RVD) is an acute

mechanism activated to counteract cell swelling in a hypo-osmotic/ hypotonic extracellular environment. RVD is achieved through the release of both ions and organic oysmolytes; this is typically achieved through the activation of K^+ channels and other anion (chloride) channels [42]. Intracellular water follows ions and organic osmolytes that are released from the cell and results in RVD.

1.4 Factors Influencing Cell Volume

In humans, exercise or even exposure to increased ambient temperature can cause many challenges to thermal homeostasis, and ultimately fluid homeostasis. When challenged, the human body will attempt to cool itself through radiant and conductive heat loss (perspiration and dry heat exchange); however, as ambient temperature increases there is a greater reliance on radiation and perspiration due to ineffective conductive and convective cooling [24]. Therefore, during exercise (especially in hot/humid environments), the body loses a significant amount of water, which has variable consequences for the different water compartments in the body. It is well documented that plasma osmolarity increases during hypohydration due to the initial decrease in plasma volume [15, 70]. In order to preserve plasma volume, fluid shifts from the ICF to the hyper-osmotic ECF [24]. In 1976, Costill et al. documented the proportion of water lost from the various compartments at different levels of dehydration. Increased levels of whole body water loss (dehydration) resulted in proportionately greater fluid loss from the ICF (Figure 1). This represented one of the first in vivo human studies to clearly demonstrate that whole body hydration status and body temperature could significantly influence cell volume.

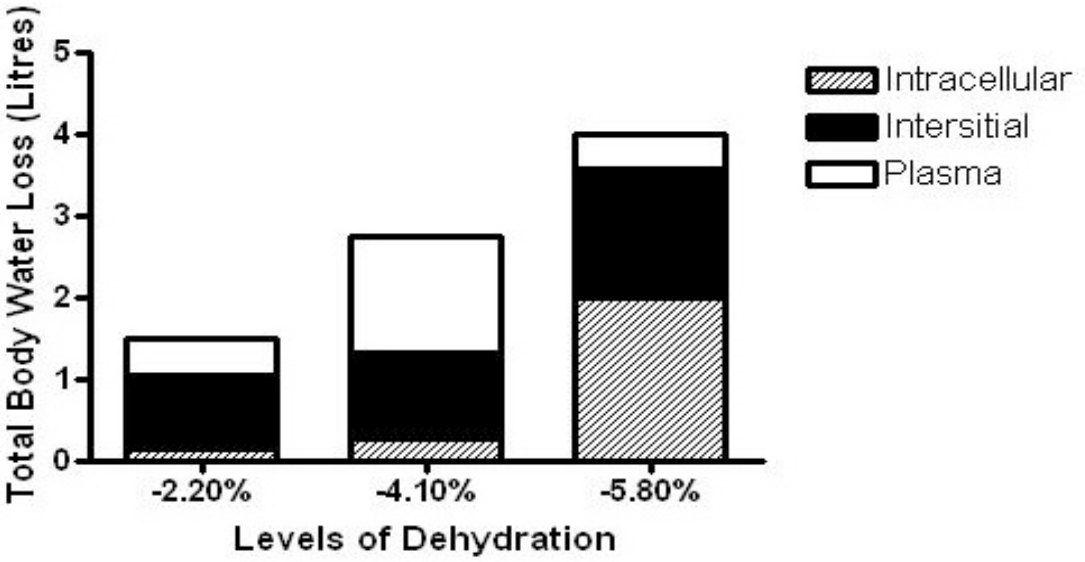

Figure 1: Proportion of water loss by compartments at different levels of dehydration (Adapted from Costill 1976)

Malnutrition, diseases and infections can also alter influence cell volume. In 1979, Barac-Nieto et al. reported that severely under-nourished males exhibited extracellular expansion and intracellular water shrinkage [6]. In addition, other hypercatabolic states such as severe burns, physical injuries, liver carcinomas etc. are accompanied by a decrease in muscle cell volume [42]. In summary, exercise, temperature and perhaps other disease states influence cell volume, typically causing cell volume to decrease. These external factors can trigger RVI activation where an influx of ions and organic osmolytes attempting to increase intracellular osmolality and restore normal cell volume.

2. Overview of Carbohydrate Metabolism

2.1 Cell Volume Influences Metabolism

In 1994, Haussinger described the Cell Swelling Theory in rat hepatocytes. When perfused with glutamine, hepatoctyes swelled for the duration of the perfusion [31]. Haussinger et al. speculated that Na^+ entered the cell via the glutamine/Na^+ co-transport, thereby creating a hypo-osmotic environment thus resulting in cell swelling [62]. The authors also discovered that protein metabolism was influenced by cell volume, as a 15% increase in cell volume inhibited proteolysis by 25% [62]. Other measurements demonstrated that cell swelling decreased glycogenolysis and glycolysis, while increasing glycogen synthesis, lactate uptake and acetyl-CoA carboxylase activity; while the opposite was true for cell shrinkage. This led the authors to believe that cell swelling was an anabolic signal (to decrease cell energy production) whereas cell shrinkage was a catabolic signal (to increase the cell energy production). Since the original findings by Haussinger, many authors have observed similar results in various models [2, 42]. More recently, our laboratory has investigated the relevance of this theory in intact skeletal muscle. Ansio-osmotic environments have been previously documented to alter both physical and metabolic characteristics in skeletal muscle [2, 19].

Antolic et al. established an in-vitro skeletal muscle model to study acute alterations in resting cell volume using isolated whole rat muscle (EDL and soleus). The rat muscles were incubated in a tissue bath where the medium was manipulated with mannitol to create three extracellular environments: an iso-osmotic environment (ISO; 290 ±10 mmol/kg), a hyper-osmotic environment (HYPER; 400 ±10 mmol/kg) and a hypo-osmotic environment (HYPO; 190 ±10 mmol/kg). A significant increase and decrease in water content and cross-sectional area was quantitatively reported in HYPO and HYPER conditions, respectively, when compared to the

ISO condition [2]. Furthermore, high energy phosphate compounds (ATP, PCr) were found to decrease while lactate content increased 4-fold under the influence of hyper-osmotic stress in EDL muscle [2]. These metabolic changes support Haussinger's hypothesis in which hyper-osmotic stress induces a catabolic response in skeletal muscle, resulting in increased flux through glycolysis and glycogenolysis (and thus an increased demand for glucose) [2]. In 2007, Farlinger followed up Antolic's experiments with the purpose of understanding the influence of resting cell volume alterations on glucose metabolism, specifically glucose uptake (unpublished thesis work) [19]. To remain consistent, Farlinger duplicated the protocol described by Antolic et al., with the addition of ^{3}H labelled 2-deoxyglucose to Medium-199 to quantitatively measure glucose uptake. The major finding was that glucose uptake was increased in HYPER environments compared to ISO and HYPO. In addition, the HYPER condition produced increased intramuscular concentrations of unphosphorylated glucose and lactate (~2-fold compared to ISO), while muscle glycogen content declined compared to HYPO and ISO conditions in EDL muscle (unpublished thesis work) [19]. These data are consistent with Haussinger's hypothesis, in which hyper-osmotic stress induces a catabolic environment and is accompanied by an increase in glucose uptake. The increase in glucose uptake may be a mechanism to restore cell volume and provide supplementary energy required for RVI.

RVI is primarily achieved through a rise in ion concentration via increased activity of the NKCC and Na^{+}/K^{+} ATPase. However, increasing particle concentration (and therefore increasing intracellular osmolality) can also be achieved through increased glucose uptake into the cell. Furthermore, mechanisms for RVI require energy, and therefore increase ATP turnover. Homeostatic mechanisms will trigger ATP producing pathways, namely glycolysis and glycogenolysis, which will also increase particle concentration (1 glucose ➔ 2 pyruvate). An increased flux through glycolysis requires additional glucose as a substrate; this is accomplished

through the breakdown of stored glycogen and increasing glucose uptake. Therefore, increasing glucose uptake seems to be an efficient strategy for cells to counteract acute decreases in cell volume. However, the exact signaling mechanisms responsible for GLUT4 translocation and activation due to hyper-osmotic stress in whole skeletal muscle remain unknown.

In 2009, Apostol et al. Suggested that there was an uncontrolled Ca^{2+} release in skeletal muscle under hyper-osmotic stress [5]. Termed calcium "sparks", spontaneous calcium release from the sarcoplasmic reticulum (SR) was observed in whole intact skeletal muscle during rest or at low activation levels. In normal excitation-contraction coupling mechanisms, a wave of depolarization travels down the transverse-tubules (T-tubules) triggering the activation of dihydropyridine receptors (DHPR) located in the T-tubule membrane. The voltage -sensing DHPR uses a mechanical link to open the ryanodine receptors (RyR) located in the SR membrane. This allows for calcium to flow down its concentration gradient and into the cytosol. Wang et al. proposed a mechanism in which hyper-osmotic stress impairs the ability of DHPR to maintain RyR's in a "closed" position, resulting in calcium leaks or sparks from the SR [5, 81]. Apostol et al. were able to support Wang's hypothesis through a spatial-temporal analysis of intracellular calcium signals in response to hyperosmotic stress [5]. These findings are an important step to uncovering a possible link between calcium signaling, osmotic stress and glucose uptake. Important signaling intermediates, AS160 and protein kinase C (PKC) are hypothesized to be active under osmotic stress and both proteins possess calcium binding domains which may play a role in regulating protein activity and possibly glucose uptake under hyper-osmotic conditions.

2.2 Glucose Homeostasis

Generally, only four grams of glucose is circulating within the blood stream of a 70kg person at any moment, however slight deviations in blood glucose can result in metabolic dysfunction, neuroglycopenia, seizure or even death [82]. Major sources of blood glucose include that endogenously produced by the liver and that exogenously consumed through the diet. The human body has established a complex control system to protect and maintain blood glucose levels between 5-6 $mmol \bullet L^{-1}$. There are two characteristics that demonstrate the importance and complexity of whole-body glucose control. Firstly, several redundancies exist in the many layers of glucoregulatory response. Glucagon and insulin are the chief hormones responsible for maintaining blood glucose, however many other hormones, including catecholamines, cortisol and growth hormone all act as a safety net to further prevent deviations in glucose homeostasis [82]. Secondly, there is a distribution of control. When the body is challenged with the consumption of a large exogenous glucose load, the range of control is not reliant on a single organ or system. Glucose removal (from circulation) occurs in two main tissues; skeletal muscle and adipose tissue. In fact, skeletal muscle is responsible for up to 75% of glucose uptake in humans [7].

Despite the attempts to maintain glucose homeostasis, many conditions threaten whole body glucose homeostasis, and perhaps the most common is diabetes mellitus. Type II diabetes is a rapidly growing disorder that is estimated to reach a global prevalence of 300 million by the year 2025 [18]. It is characterized by the inability to remove glucose from the blood resulting from dysfunctional insulin signaling mechanisms (insulin resistance) in skeletal muscle and adipose tissue. It is well established that insulin and muscle contraction are two primary stimulators of responsible for glucose uptake in skeletal muscle. Skeletal muscle is the primary and most abundant organ for glucose uptake, and therefore plays an important role in glucose homeostasis. The principle glucose transporter in human skeletal muscle is glucose transporter

4 (GLUT4). GLUT4 is one of a family of 12 facilitated monosaccharide transporters (GLUT 1-12) [33]. Other monosaccharide transporters display different characteristics in terms of tissue expression and substrate specificity. For example, GLUT1 is widely expressed in all tissues with a low capacity for glucose transport, while GLUT 5 and 11 are fructose transporters [33]. Nevertheless, GLUT4 is the chief transporter in skeletal muscle, accounting for approximately 60-70% of total glucose uptake in unstimulated (insulin) isolated skeletal muscle [64].

Individuals with diabetes lack the ability to take up blood glucose due to impaired insulin signaling mechanisms. It is hypothesized that insulin, contraction and osmotic stress, stimulate GLUT4 translocation through independent signaling mechanisms. Signaling mechanisms via insulin and contraction have received significantly more attention in the literature and the signaling mechanisms seem to be relatively well understood. In contrast, the signaling mechanisms involved in osmotically stimulated glucose uptake have received very little attention and require further research. Therefore, a greater understanding of all signalling processes involved in glucose uptake, including osmotic stress, could potentially have implications for the management of type II diabetes. Delineation of all glucose uptake stimulatory pathways could potentially lead to new therapeutic targets, and pharmacological interventions that could facilitate better glycemic control in the diabetic population.

2.3 GLUT4 translocation

It is important to understand the process of GLUT4 translocation to identify points of integration by stimulators and possibly signaling proteins. Insulin is the most well known of the stimulators and will therefore represent the majority of information in this section. However, GLUT4 recycling seems to respond similarly to both contraction and hyper-osmotic stress [36, 60].

GLUT4 cycles to and from the sarcolemma through exocytosis and endocytosis. In basal (unstimulated) conditions, the distribution favours the endocytotic arm, sequestering GLUT4 in its intracellular compartments. Microscopy has localized intracellular compartments into a perinuclear region and a few distinct regions throughout the cytosol [18]. Newly endocytosed GLUT4 merge with each other to form sorting endosomal compartments. Figure 2, illustrates the many fates of a GLUT4 vesicle as it enters the cell. Contents of the sorting endosomal compartments appear to dissociate into endosomal recycling compartment or mature into later endosomes and lysosomes [33, 47]. Downstream compartments in the cytosol have yet to be fully characterized, however the end product is known as GLUT4 storage vesicles [18]. Figure 2 indicates various points of GLUT4 recycling that may be regulated by insulin stimulation. Dotted arrows indicate hypotheses that have yet to be verified through definitive scientific experiments. It has been well established that insulin signaling rapidly increases GLUT4 recycling to favour the exocytotic arm, with minimal change to the endocytotic arm [18, 77]. This results in a shift in steady-state distribution, favouring translocation towards the plasma membrane, therefore increasing the concentration of glucose transporters at the cell surface.

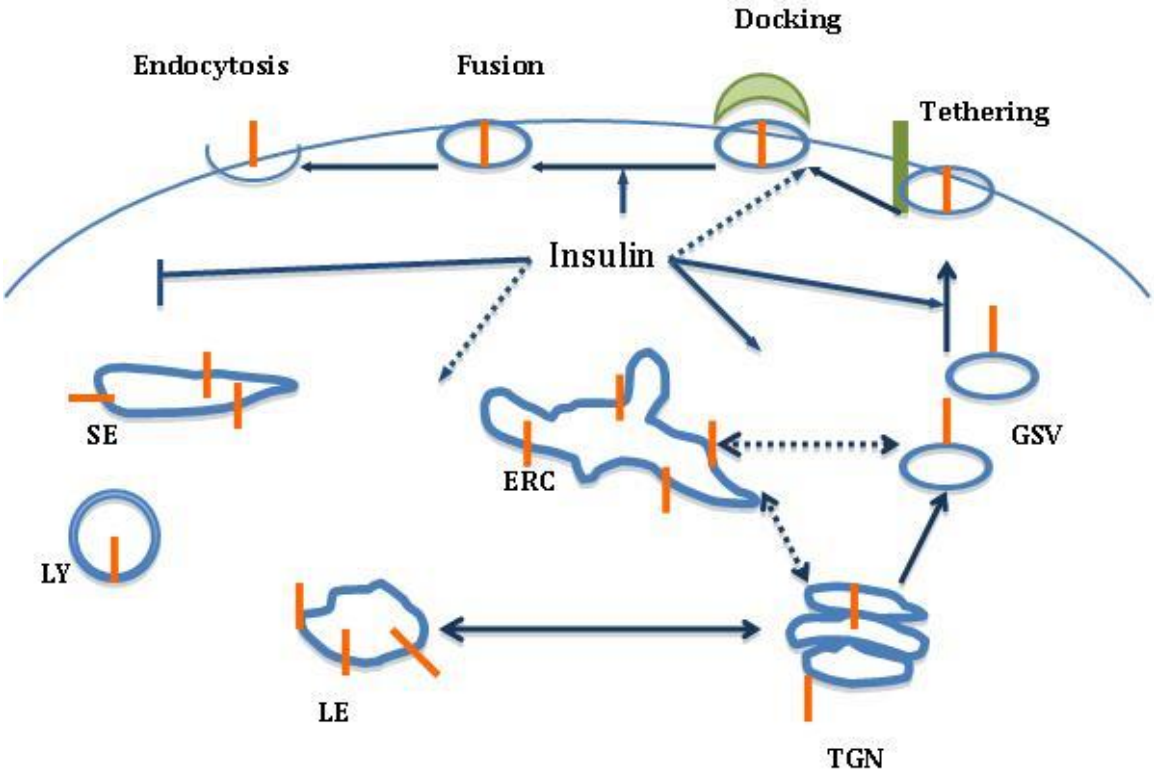

Figure 2: GLUT4 continuously recycles to (exocytosis) and from (endocytosis) the sarcolemma of muscle cells. Newly endocytosed GLUT4 transporters are initially sequestered into sorting endosomes (SE) and are either shuttled towards endosomal recycling compartments (ERC) or gradually mature to later endosomes (LE) and lysosomes (LY). The trans-Gogli network (TGN) is hypothesized to interact with ERC to generate glucose storage vesicles (GSV) allowing GLUT4 translocation to the plasma membrane. Insulin can also influence various steps within GLUT4 recycling. Solid arrows indicate known actions, whereas dashed arrows illustrate current hypothesises (Adapted from Huang 2007).

Conversely, muscle contraction and energy deprivation have been shown to reduce GLUT4 endocytosis thereby increasing GLUT4 on the membrane surface [39].

Rudich and colleagues have proposed two mechanisms to describe enhanced GLUT4 exocytosis in L6 muscle culture: the "Push" and "Pull" mechanisms [64]. The "pull" refers to actin filament remodelling upon stimulation. Actin remodelling can be thought of as building scaffolding for GLUT4 vesicles to travel on. As early as three minutes after insulin stimulation, actin begins to form mesh-like structures causing ruffles and ridges allowing GLUT4 vesicles to tether or attach and "pull" themselves towards the cell surface [64]. Currently, it is debated as to whether actin remodelling is essential for all types of stimuli [64]. The "push" mechanism involves the acceleration of GLUT4 recycling within the endosomal compartments. At steady-state, GLUT4 pools are found to co-localize with the endosomal recycling compartments and golgi organs. From here, GLUT4 is thought to exit the endosomal recycling compartment's and begin translocation towards the cell membrane as glucose storage vesicle (Figure 2). Foster et al. were able to measure the transit time (defined as the time between the arrival and exit of GLUT4 in the endosomal recycling compartments) under insulin stimulation in myoblasts [20]. Results showed that insulin reduced the transit time from 20 minutes to 10 minutes, ultimately forming the "push" hypothesis [20].

The endocytotic arm of GLUT4 translocation has received much less attention in the literature, however, there have been several mechanisms identified for the internalization of GLUT4 under various stimuli and in various tissue. Antonescu et al. determined two major routes for GLUT4 to be internalized in myoblasts and myotubes under insulin and hypertonic stimulation: a clathrin/dynamin-dependant route and a cholesterol/dynamin-dependent route [3]. Clathrin-mediated endocytosis is initiated by various light and heavy chain clathrin proteins

assembling in a shallow invagination at the surface, creating a clathrin coated pit. The clathrin coated pit gradually deepens and envelops the GLUT4 vesicles, a process facilitated by dynamin, transferrin and several other proteins [4, 47]. Once the membrane is completely enclosed, the clathrin coated GLUT4 vesicle is internalized as sorting endosomes and mature into later endosomes and endosomal recycling compartments.

Upon various stimulations, it is hypothesized that a GLUT4 vesicle undergoes several regulated steps for glucose trafficking. GLUT4 vesicles have been documented to tether, dock and fuse with the plasma membrane prior to glucose uptake [33, 39]. During the tethering phase, recent research suggests the involvement of α-actin-4, a protein that can bind GLUT4 to actin filaments [39]. Remember, actin remodelling is the basis of Rudich et al. "pull" mechanism for enhancing GLUT4 exocytosis; therefore α-actin-4 is an important protein to allow GLUT4 to interact with actin remodelling. Syntaxin 4 and its vesicle associated membrane protein-2 (VAMP2) are members of a family of soluble nitrogen ethylmaleimide sensitive factor (NSF) attachment proteins (SNARE) that are functionally required for the majority (~70%) of insulin-stimulated glucose uptake [64]. SNAREs can be divided into two categories, vesicle (v-SNARE) and target (t-SNARE) SNAREs. Simply, v-SNAREs are incorporated into the membrane of a transporting vesicle while t-SNAREs are bound onto the membrane of target tissues. v-SNAREs, Syntaxin 4 and VAMP2, seems to be specific to a specialized subpopulation of GLUT4 vesicles. More specifically, it is thought that VAMP2 is specific to insulin-stimulated "pools" of GLUT4 [64]. Interestingly, VAMP2 cleaving toxins (tetanus toxin; TeTx) do not affect GLUT4 trafficking in response to a hypertonic sucrose stimuli. This suggests that insulin and osmolality stimulate glucose uptake through diverse mechanisms and non-similar pools of GLUT4's. The tethering, docking and fusion phase are not considered secondary responses to GLUT4 stimulation. In fact, they are part of the primary response that may receive direct signals from the insulin receptor

substrate (IRS). The exact mechanisms of the tether/dock/fuse phases are still currently debated.

Recent research has shown that increased GLUT4 translocation alone does not necessarily equate to increased glucose uptake. In 2001, Somwar, Klip and colleges observed a consistent discrepancy between the magnitude of stimulation, the rate of glucose uptake and the rate of GLUT4 translocation [73]. Literature has shown that low concentrations of wortmannin (<10mM) inhibited glucose uptake without disrupting the timing and number of GLUT1's and GLUT4's translocated to the membrane [73]. The authors suggested graded levels of GLUT4 activity may account for the discrepancy between GLUT4 translocation and glucose uptake. Using insulin stimulation, Klip et al. determined that p38 mitogen-activated protein kinase (MAPK; a downstream target of the insulin) can intrinsically activate GLUT4 protein preceding GLUT4 translocation in L6 myotubes [50, 73]. Two possible mechanisms have been proposed for regulating GLUT4 activity: GLUT4 phosphorylation and/or a ligand binding mechanism [50]. GLUT4 contains one site for phosphorylation; in basal conditions, there is a larger proportion of phosphorylated than unphosphorylated GLUT4 [50]. Moreover, the phosphorylated state of GLUT4 is inversely proportional to glucose uptake [50]. Taken together, this may suggest a downstream phosphatase action by known stimulators. The ligand binding mechanism presents two possibilities, the binding of an activator or the release of an inhibitor upon stimulation. Currently, the literature endorses the latter option in cell culture, as the cytosolic C-terminus of GLUT4 is more accessible to antibodies after insulin stimulation than in its basal state [50].

GLUT4 recycling is heavily regulated and is a critical factor in the rate of glucose uptake in skeletal muscle. Stimulators (i.e. insulin, contraction and osmotic stress) of glucose uptake

seem to have multiple regulatory inputs in the GLUT4 recycling pathway. Stimulators can enhance the activity of exocytosis or even decrease the activity of endocytosis. Moreover, GLUT4 activation can be regulated apart from GLUT4 translocation, however the majority of the current literature has been investigated through insulin. Limited research is available to verify the actions of other stimulators in whole intact skeletal muscle.

3. Signaling Proteins Implicated in Glucose Uptake

This section represents a brief introduction into some of the common signaling cascades and proteins that have been described to have an association with glucose uptake. The following proteins are common to insulin and contraction stimulated glucose uptake and may be involved in hyper-osmotically stimulated glucose uptake. Complete descriptions of the detailed signaling pathways of glucose uptake will be provided in section 4.

3.1 Akt/PKB

Three (1,2 and 3) mammalian isoforms of Akt/protein kinase B (PKB) have been identified and are all stimulated by insulin via PI3-K [77, 80]. Akt1 and 2 are expressed in adipose tissue and skeletal muscle and Akt3 is also present in L6 and 3T3-L1 cell culture tissues [77]. Interestingly, Akt2 knockout mice display severely impaired glucose uptake, while Akt1 knockouts do not display any obvious insulin resistance [83]. Thus far, Akt2 is known to be responsible for metabolic actions in the body, while Akt1 is thought to facilitate growth-promoting signals and has little metabolic consequence. It is hypothesized that the enzyme is phosphorylated on $Thr^{308/309}$ of its activation loop by PDK1 (phosphotidylinositol dependent kinase 1) [77]. Akt also contains a second phosphorylation site, $Ser^{473/474}$, however; its role is not clear. It has been speculated that serine phosphorylation precedes $Thr^{308/309}$ phosphorylation and that Akt may require dual phosphorylation to be activated [77]. Akt is proposed to have multiple regulatory outputs to promote glucose uptake, rather than relaying a signal down a solitarily cascade. In fact, Akt is known to interact with over 35 various substrates involved in various survival and apoptotic processes [18]. In regards to glucose uptake, the more relevant actions of Akt include both the acceleration of endosomal transit of GLUT4, and regulation of vesicle fusion between SNARE complexes and the plasma membrane [77].

3.2 AS160/TBC1D4

AS160, also known as TBC1D4, is an Akt substrate that was first successfully identified in 2002 [37]. Although it was originally thought to be an exclusive substrate for Akt, it now appears that other kinases, like AMPK, are capable of phosphorylating and deactivating AS160 [9]. AS160 is a Rab-GAP (GTPase activating protein) that is considered the link between Akt and GLUT4 translocation. At rest, AS160 is highly active suppressing Rab proteins found on glucose storage vesicles. Upon stimulation, AS160 releases its inhibition on glucose storage vesicles - bound Rabs, allowing glucose storage vesicles to be loaded with GTP and transport GLUT4 to the cell surface [13]. AS160 appears to possess at least eight different phosphorylation sites, however, the roles of these different sites have yet to be definitively identified [13, 59, 67]. Sano et al. have identified phosphorylation sites at Ser^{318}, Ser^{341}, Ser^{570}, Ser^{751}, Ser^{588} and Thr^{642} in mouse AS160 [67] and the phosphorylation of these various sites appears to depend on the type of stimulus [13]. For example, insulin stimulated activation of Rab proteins have been observed to be mediated through phosphorylation of Thr^{642} site, while pharmacological stimulation of AMPK has been demonstrated to increase Ser^{237} phosphorylation [59, 66]. Interestingly, mutations at four of the various phosphorylation sites (including Ser^{588} and Thr^{642}) have been observed to inhibit insulin stimulated GLUT4 translocation [59, 67]. Furthermore, over expression of a mutated form of AS160 (AS160-4P) has lead to a significant decline in both insulin (~30%) and contraction (~40%) stimulated glucose uptake in skeletal muscle [41, 66]. Therefore, it appears that AS160 phosphorylation at some of its phosphorylation sites decreases AS160 activity which then allows for increased GLUT4 translocation. However, further work is required to determine the role of all of the possible phosphorylation sites on AS160.

The human genome possess over 50 Rabs and Rab-GAPs, reflecting the specificity required for such an interaction [66]. Over a dozen different Rab proteins have been found to

be associated with GLUT4 vesicles, but the key players appear to be Rab 2A, -8A, -8B, -10, 1-1 and -14, conversely their specific functions have yet to be fully understood [34, 66]. Interestingly, AS160 contains a region in a Rab-GAP domain (amino acids 834-857) that is about 58% identical to a calmodulin-binding domain (CBD) within Drosophilia protein Pollux [41]. Both human and Drosophilia peptide sequences contain key residues for calmodulin / calcium association. This association could serve as a potential mechanistic link between calcium and glucose transport involving AS160 and possibly calmodulin.

3.3 AMPK

Adenosine-5'-monophosphate protein kinase (AMPK) is a hetrotrimeric protein composed of a catalytic α subunit and two regulatory subunits, β and γ [52]. Each subunit has 2 or more isoforms. $\alpha 1$ and $\alpha 2$ are functionally considered the most important isoforms, where $\alpha 1$ is widely expressed in almost all tissue and $\alpha 2$ is the predominately found in the liver, heart and skeletal muscle. In skeletal muscle, AMPK acts as a sensor for energy status within the cell and is allosterically regulated by AMP/ATP and Cr/PCr ratios. Allosteric activation (by AMP) is required to allow phosphorylation at Thr^{172} by other upstream kinases (LKB and CaMK), leading to the activation of AMPK [52]. Moreover, AMP binding to the $\alpha 2$ causes a conformational change to protect Thr^{172} from dephosphorylation [78]. Activation of AMPK activity increases as AMP levels increase during exercise and/or metabolic stress. Examples of metabolic stress include osmotic stress, hypoxia, ischemia, thermal shock, inhibitors of glycolysis and mitochondrial uncouplers [52]. Therefore, it is logical that activation of AMPK stimulates ATP-producing pathways (glycolysis, glycogenolysis, fatty acid oxidation), while also suppressing ATP-consuming pathways (glycogen synthesis) [32, 52].

When considering osmotic stress, AMPK could be a potential candidate for activation

based on the metabolic influences of hyper-osmotic stress. HYPER extracellular environments lead to decreases in cell volume, decrease in energy status and an overall catabolic state within cells [2]. Activation of AMPK would theoretically increase the activity of ATP generating pathways in order to meet the increased energy demands required to cope with the osmotic stress. Once again, taking up glucose not only contributes to RVI through increasing omsolality, it also provides available substrate for glycolysis. Therefore, it would be logical that AMPK could play a role in regulating osmotically induced glucose uptake [32, 52, 54].

3.4 ERK MAPK

All eukaryotic cells exhibit multiple mitogen activated protein kinase (MAPK) pathways that regulate a wide variety of cellular activities that range from mitosis to cell apoptosis. To date, five distinct groups of MAPK have been characterized in mammals: extracellular signal-related kinases 1 and 2 (ERK1/2); c-Jun amino-terminal kinases (JNK) 1,2 and 3; p38; ERK 3/4 and ERK5 [63]. Each group of MAPKs belong to a family of three evolutionary conserved kinase sequences: a MAPK, a MAPK kinase (MAPKK) and a MAPKK kinase (MAPKKK). Figure 3, illustrates the family of cascades for each of the MAPK groups. Generally, MAPKs are responsive to a diverse set of stimuli, however not all MAPKs respond to each stimulus to the same degree. ERK1/2 may have a possible role in hyper osmotic induced glucose uptake signalling as it has been shown to responsed to a diverse range of extracellular stimuli including mitogens, growth factors and cytokines [63, 65]. Catalytic activity of ERK1 is achieved through dual

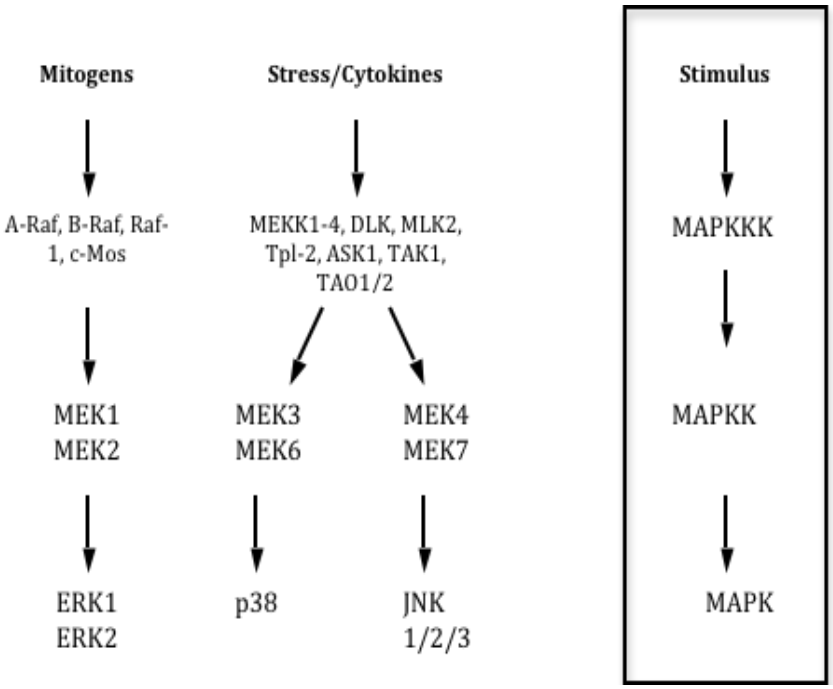

Figure 3: Family of extracellular related kinases (Adapted from Roux 2004)

phosphorylation of Thr^{202} and Tyr^{204} while ERK2 catalytic activity is achieved when dually phosphorylated at Thr^{185} and Tyr^{187} [25]. Activation of ERK1/2 upstream kinases (Raf proteins) are not fully understood, however, it is known that multiple phosphorylation events of Raf proteins at the plasma membrane are required for activation [63]. In 2002, Sajan et al. proposed that a non-receptor tyrosine kinase, proline-rich tyrosine kinase-2 (PYK-2) is responsible for activating Raf and other MAPKKK in the ERK family. Using a series of inhibitors in 3T3-L1 cells and L6 myotubes, Sajan et al suggested a pathway where PYK-2 activates Raf proteins which subsequently activates ERK1/2. This in turn increases aPKC activation and eventually results in increased GLUT4 translocation [65]. They also demonstrated that PI3-K and PDK activation did not influence sorbitol induced-PKC activation. Based on these observations, it is plausible that that hyper-osmotic stress could lead to phosphorylation and activation of ERK1/2, resulting in an increase in glucose uptake in the absence of PI3-K and other insulin-signaling proteins. Therefore, future research should investigate the possible role of this protein in hyperosmotic induced glucose uptake.

3.5 Protein Kinase C

The protein kinase C (PKC) family of serine/threonine proteins is responsible for many cellular functions including cell growth, proliferation and apoptosis. This family is subdivided into three major classes: conventional (cPKC), novel (nPKC) and atypical (aPKC). These distinctions were established based on the protein composition and ability to bind calcium and lipids. cPKC comprise the α, βI, βII and γ, while nPKC includes δ, ε, η and θ isotypes and aPKC consist of the ζ and ι/λ isotypes. cPKCs are composed of N-terminus regions consisting of C1 and C2 binding domains. The C1 domain is responsible for binding second messenger diacylglycerols (DAGs) while the C2 domain binds calcium as a second messenger. nPKCs have a functional C1 domain, but a C2 variant that does not bind calcium, making them calcium-insensitive. Similarly,

aPKC does not have a C2 binding site and a C1 domain that does not bind DAG, making these isotypes both calcium and DAG insensitive [10, 26].

PKCα is considered the dominant isoform of the cPKCs. PKCα is synthesized near the membrane in the cytoplasm where it is unphosphorylated and inactive. PKCα is activated by a two-step mechanism; first, it gains catalytic potential via the phosphorylation of in its activation loop (Thr^{497}), and this in turn autophosphorylates two additional motifs: Thr^{638} and Ser^{657}. After becoming catalytically competent, the protein is released into the cytoplasm primed for phase two of activation. Full activation requires the binding of diacylglycerol to the C1 domain, or the binding of calcium and phosphatidylserine to the C2 domain. PKCα is down-regulated by phosphatases and desensitizing agents such as heat shock protein 70 [10].

In summary, cPKC activation is partially facilitated by calcium, while calcium has been reported to partially induce glucose uptake [38, 54], and hyper-osmotic stress has been found to produce calcium sparks. Collectively, these separate observations can be interpreted to suggest that hyper-osmotically induced calcium release may lead to an increase in glucose uptake via cPKC [5]. Clearly, further research is warranted to better understand the interaction of these various signaling processes.

3.6 Time Course for Signaling Cascades

Due to the transient nature of cell signaling and the multiple steps involved in signaling processes, phosphorylation and dephosphorylation of various proteins likely occurs at varying time points. There has been limited work investigating the specific time course of signaling with osmotic stress. In 2007, Thong et al. used CHO-IR cell culture to determine the phosphorylation levels of AS160 in response to osmotic shock [76]. CHO-IR cells were exposed to 0.45 mM sucrose for 30 minutes, and phosphorylation of AS160 was significantly higher when compared

to basal levels. Similarly, Sano et al. incubated 3T3-L1 cell culture in 160nmol/L insulin for 30 minutes [67]. Results were similar to that of Thong, in which AS160 phosphorylation was significantly higher at 30 minutes compared to basal levels. Taken together, both studies demonstrate that AS160 phosphorylation was detectable within 30 minutes of stimulation.

Chen et al. used 3T3-L1 cell culture to determine the effects of osmotic shock on insulin signaling proteins, mainly, Akt [11]. Osmotic shock was induced by incubating the cell culture in 600mM of sorbitol for 30 minutes. The authors were successful in eliciting the hypothesized results for Akt and the insulin signaling cascade. In addition, Bruss et al. used rat epitrochlearis to determine the effects of 120nmol/L insulin on Akt phosphorylation [9]. Akt phosphorylation was significantly increased (from basal levels) within 10 minutes of stimulation and remained elevated for the entire 60 minute incubation. Thus, it appears that phosphorylation of Akt occurs rapidly with both osmotic shock and insulin stimulation, and is likely detectable within 30 minutes of stimulation.

Hayashi et al. hypothesized that AMPK was the central mediator of insulin-independent glucose transport during osmotic stress [32]. Rat epitrochlearis muscles were incubated in 120mmol/L sorbitol (~120 mmol/kg) for 40 minutes. AMPK activity was significantly higher at 40 minutes compared to basal, unstimulated controls. Furthermore, Williamson examined the phosphorylation time course for AMPK in C1C12 cell culture under 2mM AICAR stimulation [84]. Cells were incubated for 15, 30 and 60 minutes and AMPK was elevated at all time points compared to basal unstimulated controls. These two studies, along with other studies done by Patel [54] and Fryer [21] suggest that AMPK phosphorylation is also rapid and likely occurs within 15 minutes of stimulation and likely remains phosphorylated beyond 60 minutes of stimulation.

Rat adipocytes were used by Sajan et al. to investigate ERK activity under osmotic stress

[65]. Cells were incubated in 300mM of sorbitol for 30 minutes. ERK activity was significantly higher than non-stimulated controls at 15 minutes of incubation and was sustained to 30 minutes. Moreover, Leng et al. used rat EDL muscle to determine the effects of 120nmol/L insulin on ERK MAPK phosphorylation [44]. A time course was published between 1 minute and 40 minutes. ERK phosphorylation seemed to peak at 20 minutes (6 fold above basal levels), and remained elevated at 40 minutes (5 fold above basal). Together, these studies suggest that ERK phosphorylation also occurs rapidly, and is likely maintained beyond 40 minutes of stimulation.

In summary, there has been limited investigation of the time course of osmotic induced activation of glucose signaling cascades. Based on the limited information it would appear that AS160, Akt, AMPK and ERK all show increased levels of phosphorylation/activation within 30 minutes of exposure to osmotic stress. However, it should be noted that various models were used to establish the described time lines and as such the timelines may not be the same for different models.

4.0 Stimulators/Regulators of Cellular Glucose Uptake

4.1 Introduction

Glucose uptake in skeletal muscle is a tightly regulated process necessary to maintain whole body glucose homeostasis. Under basal, unstimulated conditions, the majority of GLUT4 vesicles are sequestered in intracellular compartments. Various stimulators such as insulin, contraction, osmotic stress, hypoxia and dinitrophenol (DNP; a mitochondria uncoupler) have been shown to redistribute GLUT4 towards the plasma membrane thereby increasing glucose uptake [18, 45, 54, 76, 77]. Most of our understanding of these mechanisms come from cell culture and adipose tissue models; the role of GLUT4 cycling in whole skeletal muscle remains to be fully confirmed [18]. By far the most studied stimulator of glucose uptake is the insulin-signaling cascade. Contraction has also gained much attention as an insulin-independent stimulator and is very attractive signaling pathway that seems to circumvent insulin resistance. Osmotic stress is a less common stimulator than the previous two, however it may present a third signaling pathway, independent of insulin and contraction. Hypoxia and mitochondrial uncoupling will not be reviewed in this investigation.

4.2 Insulin Stimulation

Insulin-induced GLUT4 translocation (Figure 4) and activation is the primary mechanism in which glucose is removed from the blood and taken up into the tissues. This has been demonstrated in cell culture, adipose tissue and skeletal muscle [11, 18-20]. Elevations in blood glucose will trigger the release of insulin from the pancreas into the blood stream. Insulin binds to the extracellular α-subunit of the insulin receptor (IR), found on the surface of adipocytes and skeletal muscle cells; this in turn results in a conformational change of the IR. This physical change causes multi-site autophosphorylation of the tyrosine residues on the β-subunit, leading

to increased tyrosine kinase activity. Consequently, the insulin-receptor substrate (IRS) binds to the IR through phosphotyrosine- binding (PTB) sites, thereby creating a high affinity binding site for effector proteins containing Src homology 2 (SH2) domains [55, 77]. The chief SH2 containing protein is the p85 regulatory subunit of type 1A phosphatidyl inositol 3-kinase (PI3-K). Interaction of the p85 subunit with IRS-1 causes activation of the p110 catalytic subunit of PI3-K. The role of PI3-K has been demonstrated to be essential from experiments utilizing the PI3-K inhibitor, wortmannin [32, 77]. Wortmannin has been shown, and used by many scientist, to lengthen insulin-stimulated GLUT4 endosomal transit time and inhibit actin remodeling required for GLUT4 translocation [77]. From here, the activated PI3-K continues to migrate towards the plasma membrane where it phosphorylates phosphatidyl inositol (3,4) diphosphate [$PI(3,4)P_2$] and converts to phosphatidylinositol 3,4,5-triphosphate [$PI(3,4,5)P_3$]. The activation of PIP_3 recruits Akt to the plasma membrane though the activation of PIP_3-containing effector protein phosphatidylinositol-dependant kinase-1 (PDK1) [77, 83]. PDK1 will then phosphorylate and activate Akt. Akt is known to control many common cellular processes which are vital to cell survival and more specifically glucose metabolism.

The next step in the insulin-signaling cascade involves a recently discovered protein known as AS160. Akt activation is known to inhibit the Rab GAP activity thereby resulting in the conversion of Rab-GDP to Rab-GTP. GLUT4 vesicles loaded with GTP are able to mobilize towards the plasma membrane and increase glucose transport [76, 77]. AS160 appears to be the last signaling protein involved in the cascade before GLUT4 translocation. Therefore, AS160 represents the definitive signal that leads to the translocation of GLUT4, and as such it is important to understand its role under various forms of stimulation such as osmotic stress.

It is also important to note that the insulin pathway bifurcates at several points along the cascade. From the most proximal end, signals from IRS-1 protein divide into a PI3-K

independent, yet parallel pathway [28, 39, 77]. This pathway involves the c-Cbl associated protein (CAP), Cbl and the GTPase TC10 and could possibly regulate GLUT4 translocation in muscle. However, the validity and function of the pathway remains debated and has only been documented in adipose tissue [18, 55]. In addition, PDK1 is known to interact with a second downstream target other than Akt, called atypical protein kinase C (aPKC). The aPKC pathway is considered an important cascade for activating motor proteins such as kinesins, which contribute to GLUT4 vesicles migration to the sarcolemma [34, 68].

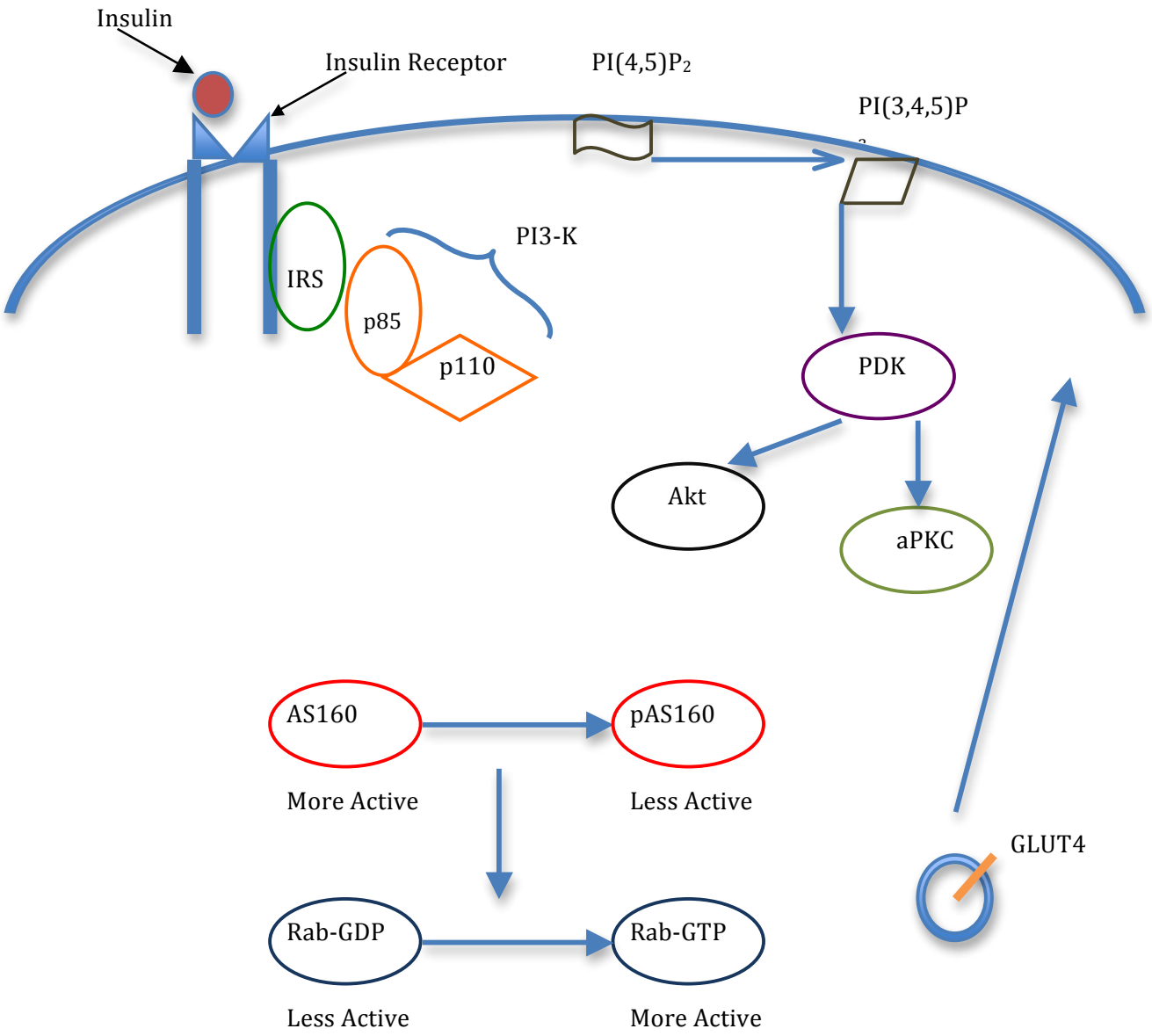

Figure 4: A schematic representation of the insulin signaling cascade in skeletal muscle. Insulin receptor substrate (IRS), phosphatidyl inostiol 3-Kinase (PI3-K), phosphatidyl inostiol diphosphate (PIP_2), phosphatidyl inostiol triphosphate (PIP_3), phosphatidylinositol-dependant kinase (PDK), protein kinase C (PKC), Akt substrate of 160 kDa (AS160). Adapted from Thong 2007

4.3 Contraction

Muscle contraction is another potent stimulator of glucose uptake for both healthy individuals and individuals with diabetes [68]. Glucose uptake during skeletal muscle contraction has been observed numerous times in the absence of insulin [17, 36, 41, 52]. Moreover, PI3-K inhibitor, wortmannin, has been shown to have no effect on contraction-induced uptake [17, 36, 68]. Interestingly, the influence of insulin and contraction on glucose transport are additive, and research has provided compelling evidence that the signaling mechanisms for insulin and contraction are partially independent and divergent. In fact, it is hypothesized that insulin and contraction stimulated signaling are initiated differently leading to independent proximal pathways, however the downstream targets may converge. Ultimately, the contraction mediated signaling cascade has gained much attention as it is a very attractive pathway to target as an alternative to possibly circumvent the deficiencies that occur with insulin resistance and type II diabetes.

Currently, there are two suggested mechanisms to explain contraction mediated glucose uptake. The first is based on the metabolic and energetic stresses placed on the cell during muscle contraction. The second suggests Ca^{2+}, as a second messenger, initiates the translocation of GLUT4 towards the plasma membrane.

By far the most popular protein-kinase associated with metabolic/energetic stress and glucose uptake is AMPK. Over the past decade, extensive research has been conducted to relate AMPK and contraction-induced glucose transport. One of the most utilized techniques to study this protein is with 5-aminoimidazole-4-carboxamide-riboside (AICAR), a pharmacological agent that can directly activate AMPK. Many scientists have documented a strong relationship between increased AMPK activity, glucose transport and muscle contraction in all tissue types

[21, 32, 36, 52, 78].

The exact signaling mechanisms involving AMPK and glucose transport have yet to be fully understood. Recent findings in cell culture propose tumor suppressor kinase, LBK1, as the major upstream regulator of AMPK [71]. Some convincing work by Thong et al. used a muscle specific LKB1 knockout (KO) mouse model to support the role of AMPK in mediating glucose uptake with contraction [76]. In their study, they reported reduced AMPK activation by AICAR and muscle stimulation in EDL from LKB1 KO's [76]. Therefore, LKB1 seems to be an essential upstream catalyst for AMPK activation, but whether it is the only kinase responsible for AMPK activation is still being debated.

The contraction-stimulated pathway is thought to converge with the classic insulin cascade downstream of AMPK and Akt. Recently, separate labs have independently demonstrated that AS160 may be a possible point of convergence, as AS160 was found to be phosphorylated during both insulin and contraction induced stimulation of glucose uptake (Figure 5) [9, 16, 36]. Phosphorylation of AS160 and AICAR-induced glucose transport was completely abolished in skeletal muscle from AMPKα2 knockout mice [78], suggesting the AS160 is a likely downstream target of AMPK. Similarly, inhibition of Akt and AS160 phosphorylation is known to reduce insulin mediated GLUT4 translocation [9, 76]. AS160 represents a possible point of convergence as it appears to be involved in both insulin and contraction stimulation of glucose uptake. It has also been suggested to be the final step before GLUT4 translocation; however, additional research is required to address this hypothesis adequately.

Another mechanism that has been suggested to possibly mediate contraction induced glucose uptake involves the released of Ca^{2+} from the sarcoplasmic reticulum (SR). Alpha-motor

neuron stimulation of skeletal muscle leads to intracellular spikes in Ca^{2+} which results in actin and myosin interaction, and ultimately force production in skeletal muscle. Caffeine is a pharmacological agent used in literature to initiate the release of Ca^{2+} without depolarization of the T-tubules or energy depletion [36, 87]. The underlying mechanism of Ca^{2+} induced glucose uptake is unknown, however, it is unlikely that Ca^{2+} directly initiates the GLUT4 transport system, since Ca^{2+} is almost immediately sequestered back into the SR, while GLUT4 transport is comparatively elevated for a prolonged period of time [36]. Alternatively, Ca^{2+} could act as a second messenger for other proteins. Two groups proteins have been identified in this context: the CaMK family consisting of CaMK I, II and III and a family known as the PKC family [36, 68]. Through an unknown mechanism, CaMK is hypothesized to facilitate Ca^{2+} stimulation of glucose uptake by enhancing GLUT4 translocation to the plasma membrane of skeletal muscle [68]. Wright et al. reported a synergistic effect between AMPK, AICAR, CaMK and caffeine on glucose uptake [86]. Introduction of KN62 (a specific inhibitor of CaMK) inhibited glucose transport stimulated by caffeine by ~66%, while inhibiting contraction-stimulated glucose uptake by approximately 50% [86]. This contradicted previous literature which reported that CaMK and AMPK stimulated glucose uptake through independent signaling pathways. Recently, Jessen et al. proposed the concept of CaMK kinase (CaMKK) being an upstream signaler of AMPK, suggesting muscle contraction can activate AMPK through both Ca^{2+} and AMP/ATP ratios [35]. Figure 6 illustrates a proposed signaling pathway where calcium could potentially regulate glucose uptake in skeletal muscle, however the mechanism is still highly debated [68].

Atypical and conventional PKCs are less studied than CaMK, however, some studies have shown muscle contraction alone activates the PKCs [36]. In addition, inhibition of aPKC (using polymoxin B) has simultaneously diminished contraction-induced glucose uptake. These results, however, should be interpreted with caution, since polymoxin B is not a specific inhibitor of

aPKC and may influence contractile properties of skeletal muscle and/or possibly influence other kinases [36]. In summary, the current literature has provided convincing evidence that contraction mediated glucose uptake converges with components of the classic insulin signaling cascade. AS160 may be the point of convergence as it influences both contraction and insulin stimulation. AMPK is generally acknowledged to be at least partially involved with contraction stimulated glucose transport, due to energy stresses on the cell. Calcium released during muscle contraction may also stimulate glucose transport through CaMK and PKC, however further research is required.

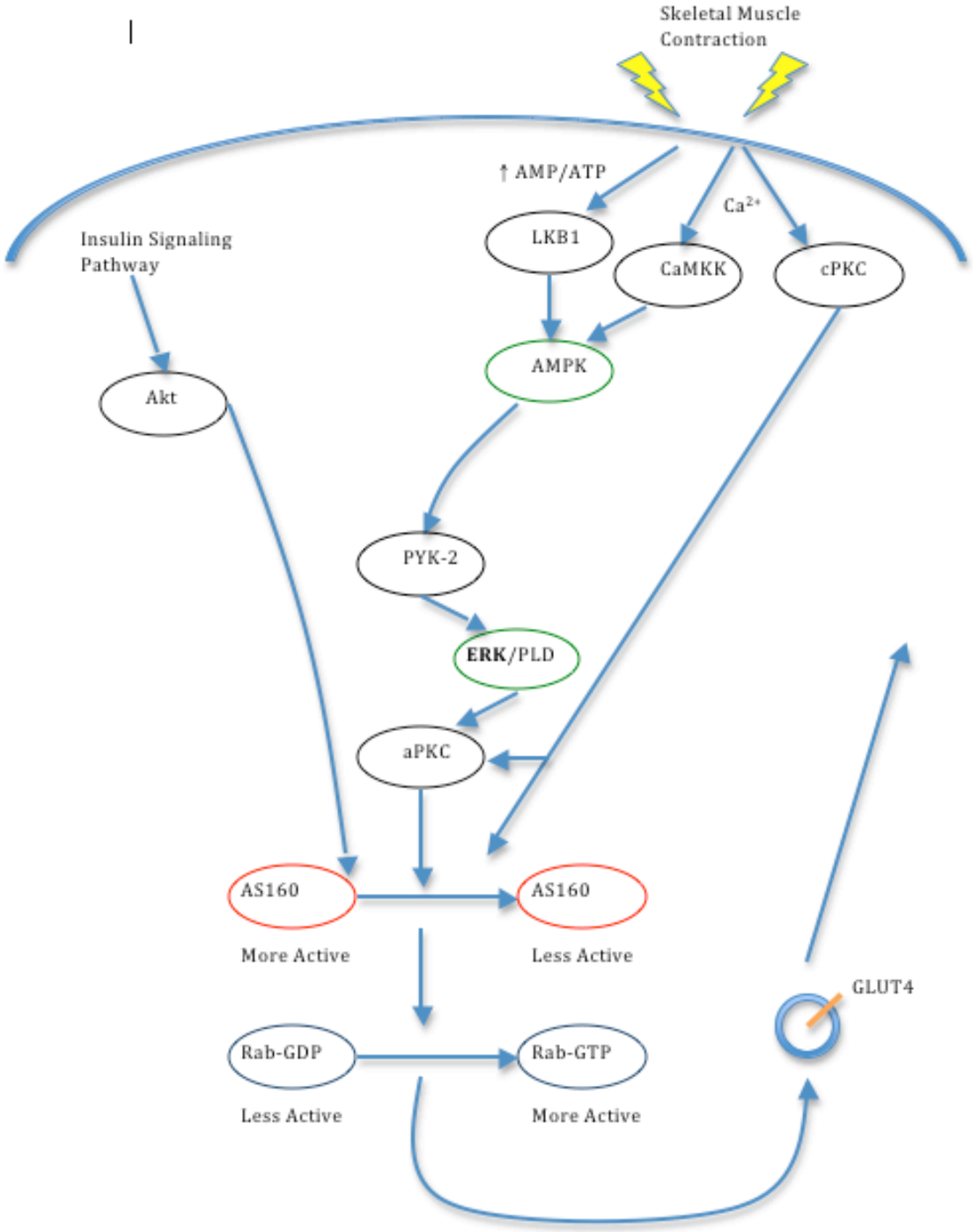

Figure 5: A schematic representation of the contraction stimulated signaling cascade in skeletal muscle. Atypical protein kinase C (aPKC), conventional protein kinase C (cPKC), Akt substrate of 160 kDa (AS160), calmodulin kinase kinase (CaMKK), AMP-activated protein kinase (AMPK), Extracellular related kinase (ERK). Adapted from Sakamoto et al 2008.

4.4 Hyper-Osmolality

In isolated whole skeletal muscle, osmolality has only been recently identified as a stimulator for increasing glucose uptake (unpublished thesis work) [19]. The majority of existing literature suggesting osmolality as a stimulator has been documented in cell culture and adipose tissue [11, 45, 65]. Recent findings suggest hyper-osmotic stress may increase GLUT4 content at the plasma membrane from various intracellular "pools" [19].

Li et al. reported that hyper-osmotic stress induced GLUT4 translocation from a "pool" other than the insulin pool in L6 myoblasts [45]. This was evident when hyper-osmolality was insensitive to TeTx cleavage of VAMP2. Recall that VAMP2, a v-SNARE is functionally required for the majority (~70%) of insulin-stimulated glucose uptake (see GLUT4 recycling). Therefore, it is possible that osmotically induced GLUT4 translocation draws from another pool, or another mechanism is utilized by hyper-osmolality to maintain GLUT4 at the plasma membrane. In 2000, Randhawa et al. reported that hyper-osmotic stress recruited GLUT4 using a TeTx insensitive, v-SNARE, T1-VAMP [60]. In this investigation, myoblasts were transiently infected with small interfering RNA for VAMP1 (T1-VAMP siRNA). This intervention lead to a robust reduction in the concentration of membrane-bound GLUT4 vesicles in response to hyper-tonicity, however, only a partial reduction was observed during insulin stimulation [60]. The authors then concluded that insulin and hyper-tonicity recruit GLUT4 from distinct pools that require VAMP2 and T1-VAMP, respectively [28, 45, 60].

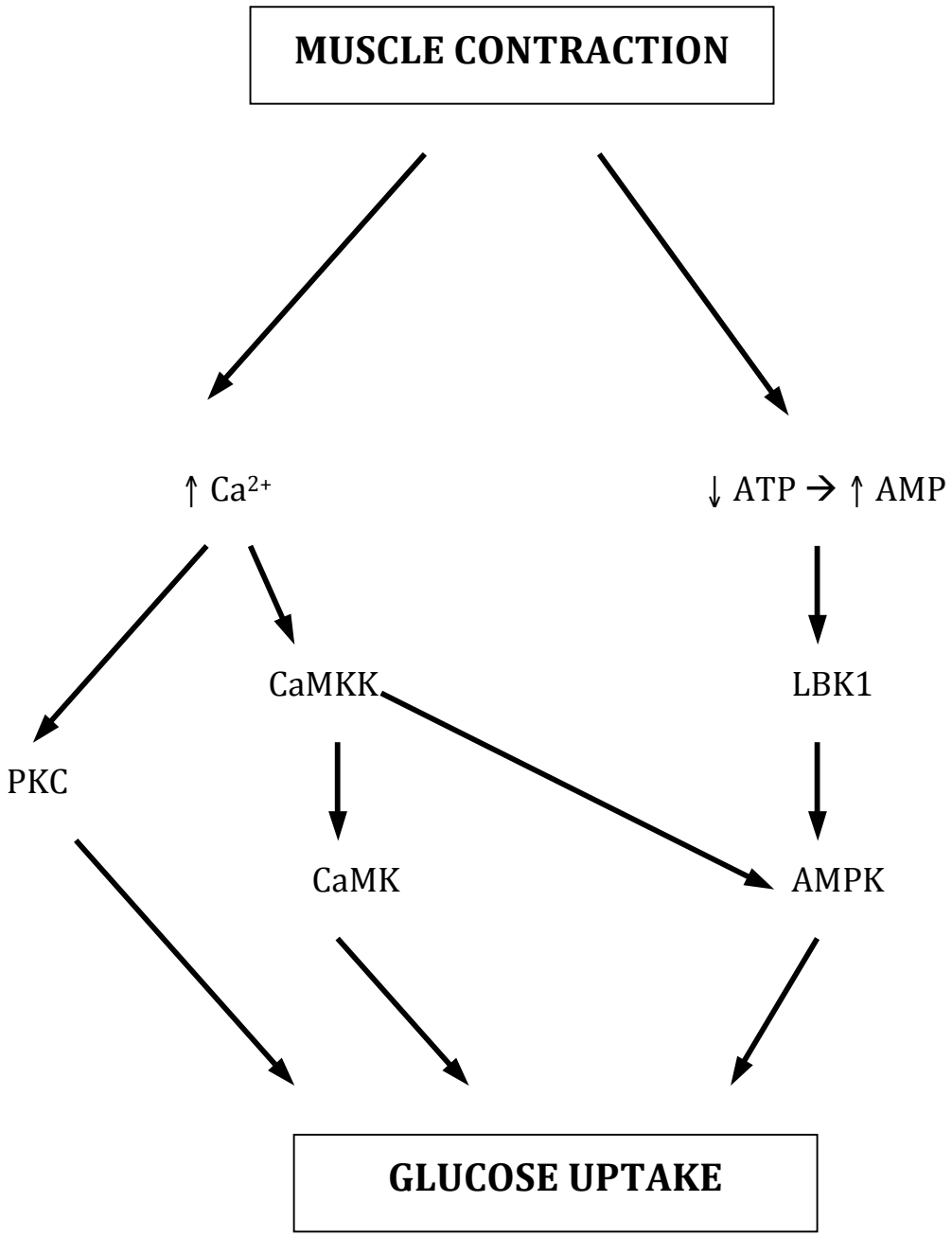

Figure 6: Proposed signaling cascade for calcium activated proteins on increasing glucose uptake (Adapted from Santos 2008)

In cell culture, Li et al. reported that hyper-osmolarity increased GLUT4 concentration at the cell membrane by abolishing GLUT4 internalization [45]. Interestingly, K^+ depletion is one technique known to prevent GLUT4 endocytosis possibly in a manner similar to what has been observed with hyper osmotic stress. K^+ depletion interferes with clathrin lattices at the plasma membrane thereby inhibiting clathrin mediated endocytosis [29]. Therefore, the concentration of surface GLUT4 should be similar when comparing hyper-osmotic stress with K^+ depletion [29, 45]. Li et al. were able to compare the two processes by first measuring GLUT4myc traffic in a 60 minute incubation period in a hyper-osmotic environment. During the 60 minutes GLUT4myc was maintained on the cell surface while K^+ concentrations diminished. The myotubes were then removed from the hyper-osmotic environment and placed in a K^+ free, iso-osmotic buffer for 30 minutes. The authors reported that GLUT4myc remained on the surface despite the iso-osmotic environment. A comparative experiment was also performed and found that removal from the hyper-osmotic environment into a K^+ containing medium significantly restored GLUT4myc internalization [45]. These results strongly suggest that hyper-osmolality and K^+ depletion can increase GLUT4 accumulation at the cell surface.

Osmotic stress can also stimulate a rise in glucose uptake through increased activation of the exocytotic arm. It is hypothesized that this mechanism is largely independent of IRS1 and PI3-K, due to insensitivity to wortmannin in both adipocytes and muscle cell culture [28]. The mechanisms regulating the response to osmotic stress in skeletal muscle have yet to be fully understood, however, osmotic stress and insulin are hypothesized to stimulate GLUT4 exocytosis through diverse signaling pathways in all tissue types [11, 45, 60, 65]. In fact, it has been documented in cell culture that insulin and hyper-osmotic stress produce partially additive gains in glucose uptake [45]. However, the order of stimulation appears to have a profound effect on the resulting glucose uptake.

Li et al. demonstrated that insulin treatment followed by osmotic stress increased sarcolemmal GLUT4 concentrations by three-fold compare to basal levels. Conversely, when insulin treatment follows osmotic stress, only a two-fold increase is seen in membrane GLUT4 concentrations [45]. These results support a previously reported concept in which hyper-osmolality leads to cellular insulin resistance [11, 28, 45]. Using 3T3-L1 cell culture, Chen et al. have documented that osmotic shock inhibited insulin signaling by maintaining Akt in its dephosphorylated state, while increasing serine phosphorylation on IRS-1 [11, 28]. During insulin stimulation, IRS-1 is phosphorylated on its tyrosine residues, leading to its activation. Serine phosphorylation is known to inhibit IRS-1 function, therefore preventing insulin-stimulated glucose uptake [28]. Therefore, osmotic stress may lead to decreases in insulin stimulated glucose uptake through inhibition of IRS-1 and Akt.

Further work has investigated the interaction of osmotic stress with other components of the insulin signaling pathway. Thong et al. used L6 cell culture with point mutations at AS160 (RK-AS160; GAP activating protein is inactive) to investigate the relationship between insulin and osmotically induced glucose uptake. It was reported that insulin and osmotically induced GLUT4 translocation were not affected by the point mutations [76]. This suggests that AS160 is not essential in insulin and osmotically induced GLUT4 translocation. Within the same study, Thong et al. examined AS160 phosphorylation in cultured Chinese hamster ovary cells with over expressed insulin receptors (CHO-IR) under hyper-osmolar sucrose stimulation. The authors reported a significant increase in AS160 phosphorylation following a 30 minutes hyper-osmotic perturbation (0.45M sucrose) [76]. Combined, these results possibly suggest that the involvement of AS160 in osmotically induced glucose transport may be tissue dependent. Another possibility is that AS160 phosphorylation is active under hyper-osmotic stress but may not be essential for GLUT4 translocation. All in all, the current literature suggests that osmotic

stress stimulates glucose uptake independently of IRS-1, PI3-K and Akt in adipocytes and muscle cell culture; while the possible involvement of AS160 remains unclear. Figure 7 illustrates possible signaling mechanisms that are proposed to stimulate or suppress GLUT4 translocation with osmotic stress.

In much of the current literature, hyper-osmotic conditions are induced through the addition of a pharmaceutical sugar alcohol agent, sorbitol, to the media. It has been demonstrated that muscle cells in culture, treated with sorbitol (hyper-osmotic condition; 600mmol/L), results in the activation of AMPK [22]. In turn, sorbitol induced activation of AMPK is thought to stimulate glucose uptake. This was further supported when over expression of a dominant-negative form of AMPK inhibited sorbitol induced glucose uptake [21, 28]. Recall that AMPK is a very common signaling protein involved when the energy status of the cell is compromised. During hyper-osmotic stress, RVI increases the energy demand of the cell and it is hypothesized that AMPK would be active under such stresses in skeletal muscle. However, limited literature exists on the role of AMPK in glucose uptake.

Signaling downstream of AMPK is still unclear (in cell culture and whole muscle) and two different pathways have been proposed. Fryer and Jessen have both suggested an important role for nitric oxide (NO) and nitric oxide synthase (NOS) in sorbitol induced glucose uptake [22, 36]. Theoretically, the activation of AMPK phosphorylates NOS thereby increasing NO production. Subsequently, NO activates the soluble form of guanylate cyclase, producing the second messenger cyclic guanosine monophosphate (cGMP). The exact mechanisms downstream of cGMP are largely unknown and require further research, however; the end result is thought to be increased GLUT4 translocation to the plasma membrane [22, 48]. Using H-2b cell lines, Fryer et al. successfully demonstrated that inhibition of either NOS or guanylate

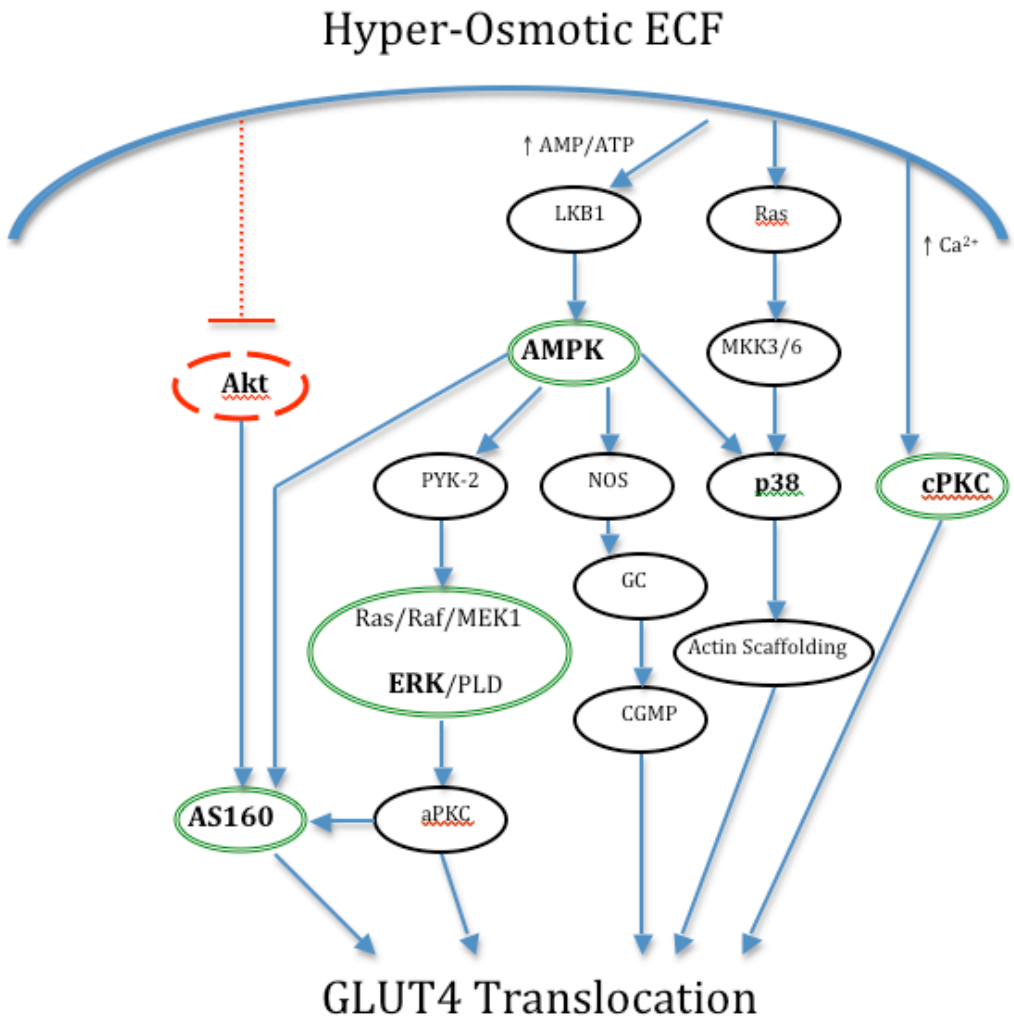

Figure 7: Illustrates the proposed pathways of signaling stimulators. Double circled proteins (AS160, AMPK, cPKC, ERK) are hypothesized to be phosphorylated under hyper-osmotic stress. Proteins in a dashed circle (Akt) are hypothesized to be less phosphorylated under hyper-osmotic stress.

cyclase significantly reduced glucose uptake stimulated by either AICAR or hyper-osmotic stress (600mmol/L of sorbitol) [22].

Another mechanism proposed to be downstream of AMPK during osmotically induced glucose uptake in adipocytes involves the activation of extracellular related kinase (ERK) [65]. Sajan et al. suggest that the activation of AMPK promotes the activation of non-receptor proline-rich tyrosine kinase-2 (PYK-2) leading to the activation of the RAS/ERK pathway [28, 65]. The ERK pathway theoretically activates phospholipase D (PLD) leading to the stimulation of aPKC, resulting in increased glucose uptake [28, 65]. Indirectly, ERK activation has been observed in skeletal muscle with hyper-osmotic stress [88]. Hyper-osmotic stress normally leads to the activation of the NKCC, however when they introduced an inhibitor of the ERK pathway, the activation of the NKCC was reduced, suggesting that hyper-osmotic stress leads to activation of the ERK pathway in muscle cell culture. Taken together is possible that the ERK pathway could be involved in osmotic stress induced glucose uptake, however, to date there has been no research investigating this possibility in skeletal muscle.

It has been suggested that mitochondrial uncoupling can also activate cPKC (via increased cytoplasmic calcium concentrations) and result in rapid glucose uptake in L6 cell culture giving further support of the involvement of calcium as a second messenger [38]. Mitochondrial uncoupling, via DNP, provokes a rise in intracellular calcium, subsequently activating cPKC through its calcium regulatory domain in muscle cells [38]. Therefore, during this investigation, cPKC is hypothesized to be involved in a signaling cascade responsible for stimulating glucose uptake. Khayat et al. reported that chelation of calcium inhibits 78% of DNP induced glucose uptake [38]. The mechanism responsible is wortmannin insensitive, therefore it is also independent from the insulin cascade. Furthermore, treatment to inhibit cPKC activation,

decreased DNP stimulated glucose uptake by 50%, and did not affect insulin stimulated glucose uptake [38]. Taken together, cPKC activation is likely to be partially responsible for observed increases in glucose uptake under what appears to be calcium mediated DNP stimulation. As mentioned previously, hyper-osmotic stress has recently been observed to cause uncontrolled calcium sparks in skeletal muscle cells [5, 81]. When combined with Khayat's research, this presents the possibility that osmotically stimulated calcium sparks could also activate cPKC, which turn could increases glucose uptake. This concept is supported by observations made in L6 cell culture, where calcium chelation and cPKC inhibition significantly reduced cell surface GLUT4 content, but had no effect on AMPK activity [54].

Research has also shown hyper-osmotic stress to increase the activity of the exocytosis of GLUT4. Exocytosis in cell culture seems to be largely dependent on AMPK, ERK, cPKC and NOS during hyper-osmotic stress, while activation of Akt, IRS1 and PI3-K are thought to be independent of osmotically induced glucose uptake. AS160's involvement in osmotically stimulated glucose uptake is largely unknown in all tissues. The vast majority of research done to date, has been reported with either adipocytes or muscle cell culture. As such, the involvement of AMPK, ERK, cPKC, AS160 and Akt are not well understood in whole, intact skeletal muscle.

5. Statement of the Problem

5.1 Statement of the Problem

Currently, it is accepted that skeletal muscle glucose metabolism is altered in response to aniso-osmotic environments [19]. Glucose uptake is significantly increased in muscles exposed to hyper-osmotic stress when compared to muscles exposed to iso-osmotic conditions and hypo-osmotic stress [19]. The signaling mechanisms responsible for increased glucose uptake under hyper-osmotic stress are not fully understood. Akt, AMPK and ERK are common proteins involved in several essential cellular processes including insulin mediated glucose uptake (Akt), cell proliferation (Akt, Erk), contraction mediated glucose uptake (AMPK) and energy regulation (AMPK). cPKC is hypothesized to be activated by free cytoplasmic calcium and appears to contribute to GLUT4 translocation to the cell surface [76]. Lastly, the phosphorylation of AS160 is directly involved with both insulin and contraction mediated glucose uptake, therefore its role in osmotically glucose uptake warrants investigation. Osmotic stress is a complicated metabolic stress for skeletal muscle, and as such multiple signalling cascades appear to be involved. Akt, Erk, AMPK, cPKC and AS160 have all been observed to have a potential role in the signalling responses to osmotic stress in various cell types, yet there has very limited characterization of these signalling processes during osmotic stress in whole skeletal muscle tissue.

5.2 Purpose

AMPK, Akt, AS160, cPKC and ERK MAPK are common proteins in the insulin and contraction signaling pathways, however their involvement in hyper osmotically induced glucose uptake remains unclear in intact whole muscle tissue. The purpose of this investigation is to investigate the phosphorylation states of these signaling proteins during 1 hour of hyper-osmotic stress in isolated rat skeletal (EDL) muscle.

5.3 Hypothesis

It is hypothesized that under hyper-osmotic stress, AMPK, cPKC and ERK will be relatively more active at the earlier time points when compared to muscles in an iso-osmotic environment at the same time points. The active forms of AMPK, cPKC and ERK are equivalent to the phosphorylated form of the proteins. In accordance with previous literature, Akt and AS160 are expected to be found in their non-active state. Therefore, it is hypothesized that the phosphorylation state of Akt under hyper-osmotic stress will be similar when compared to the iso-osmotic environment. On the other hand, decreasing AS160 activity is achieved through the phosphorylation of the protein, therefore it is hypothesized that under hyper-osmotic stress, AS160 phosphorylation will be increased as compare to muscles in an iso-osmotic environment in the later time points of incubation.

6. Methodology

6.1 Animals

A total of thirty-three male Long Evan rats (Charles River Laboratories, St. Constant, QC) were used for this investigation. Young rats (30.7 ± 3.7 days old; 128.6 ± 21.7g) were used to ensure shorter diffusion distances within the incubated muscles due to the smaller muscle size in the animals. All animals were housed within Brock University's Animal Care Facility with 4-6 rats per cage. All animals had *ad libitum* access to both food and water (5012 rat diet, PMI Nutrition Inc. Brentwood, MO) prior to experiments. Furthermore, the animals operated on a 12:12 hour light-dark cycle at a constant ambient temperature of 22°C. All procedures were approved by the Brock University Animal Care and Use Committee (ACUC) and conformed to the Canadian Council on Animal Care (CCAC) guidelines.

6.2 Osmotic Conditions

The model used in this study had been previously validated by Antolic et al [2]. Briefly, isolated whole rat muscle were incubated in a tissue bath and submerged in a medium (Sigma medium 199 Sigma Aldrich St. Louis MO, USA; M4530; Appendix I) designed to preserve physiological conditions of ECF. The incubation medium was continually perfused with a gas mixture of 95%-O_2-5%-CO_2 and temperature was maintained at 30 ±2°C. Within the bath, each muscle was resting under 1 gram of tension. Based on previous literature, 8mM of extracellular glucose induces half maximal rate of glucose uptake in rat skeletal muscle [56, 85]. Thus to achieve optimal rate of glucose uptake, D-glucose (Sigma Aldrich St. Louis, MO, USA; G-8270) was added to elevate the glucose concentration of the Sigma medium (ECF) from 5mM to 8mM. The medium was further manipulated with mannitol (Sigma-Aldrich St. Louis, MO, USA; M-9546; Appendix II) to create two extracellular environments: an iso-osmotic environment (ISO; 290

±10 mmol/kg), and a hyper-osmotic environment (HYPER; 400 ±10 mmol/kg). Osmolality of each solution was validated using a VAPRO pressure osmometer (VAPRO5520, Westcor, Logan, UT).

6.3 Muscle Extraction

Prior to the surgical procedure, rats were anaesthetized with sodium pentobarbital (55mg/kg) via interperoneal (IP) injection. Once the animal became unresponsive to physical stimuli muscle extraction began by removing the skin from the distal hindlimb. A small incision between the lateral patella to the lateral malleolus was made to separate the fascia of the superficial muscle groups, thereby exposing the deeper muscles of the hindlimb. Once the EDL was identified, sutures (4-0 Silk) were fastened at each tendon in situ, and the muscles were then excised. Sutures were used to secure muscles to the organ bath (Radnoti Glass Technology Inc., Monrovia, CA) containing approximately 15 ml of the Sigma media. The EDL was hung from a force transducer (Grass Telefactor, West Warwick, RI) and randomly placed in one of two conditions: ISO and HYPER (Figure 9). Within the ISO and HYPER groups, muscles were incubated for 30, 45 or 60 minutes (n=10 per group). Following incubations, each muscle was flash frozen in liquid nitrogen and stored at -80°C for subsequent analysis (Figure 9). A group of five non-incubated muscles (NON) were excised and immediately flash frozen in liquid nitrogen and stored at -80°C and later used for metabolite analysis. EDL muscles were strategically excised when rats were approximately 29-30 days old. This coincided with body masses of ~110-140g and this served two purposes. Firstly, at about 30 days old, muscle fibre types were fully matured and differentiation between slow and fast twitch muscle was ensured [14].

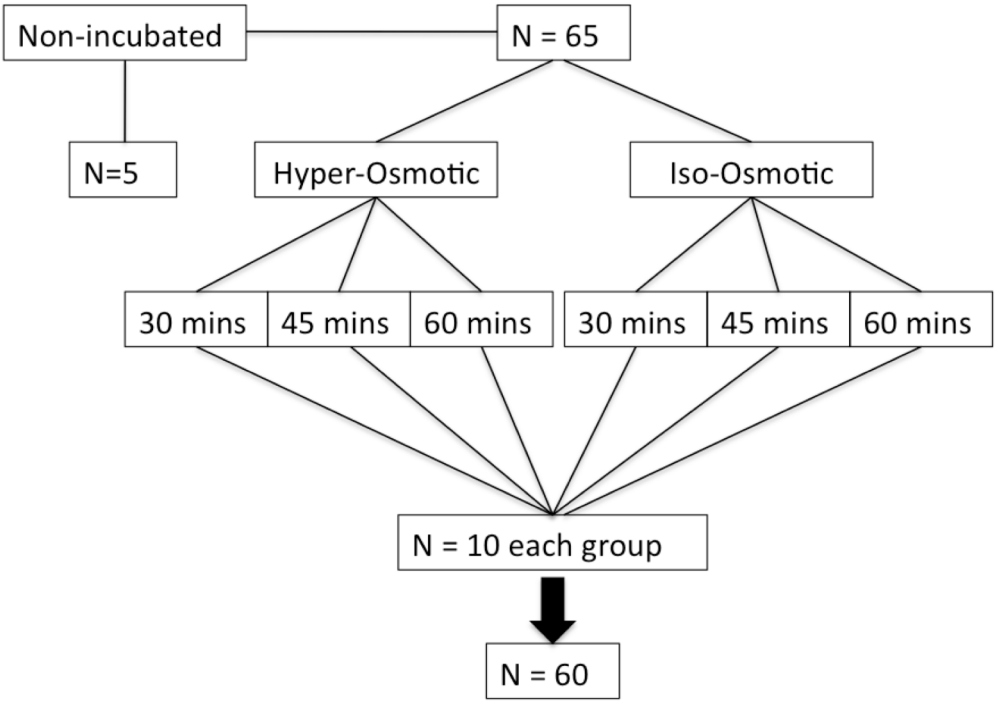

Figure 8: A breakdown of the experimental groups,
N = single EDL muscle.

6.4 Metabolite Analysis

Adenosine triphosphate (ATP) and phosphocreatine (PCr) were measured to verify the viability of the muscle incubations. Small pieces of muscles from three samples per time group were randomly selected for metabolite analysis. Approximately half of each muscle sample was chipped off and lyophilized for ~18 hours. Each sample was then powdered and any visible connective tissue or blood was removed. Metabolites were then extracted using 0.5M perchloric acid and later neutralized with potassium bicarbonate. Enzymes such as G-6-P dehydrogenase, HK and creatine kinase were added to samples along with excess substrates to create environments where ATP and PCr were limiting substrates. ATP and PCr concentrations were indirectly measured through fluorescence of nicotinamide adenine dinucleotide phosphate (NADPH). Fluorometric techniques originated from Harris et al. [30], were modified by Green et al. [27] and further adapted in our lab by Antolic et al. [2]. Detailed methods can be found in Appendix III.

6.5 Protein Quantification: Western Blotting

Frozen muscles were homogenized by hand in an ice-cold lysis buffer (~14 $\mu l \cdot mg^{-1}$ wet wt); 250mM sucrose; 100mM KCl; 5mM EDTA; pH 6.8) along with a protease and phosphatase inhibitor solution (Roche Diagnostics, Mannheim, Germany). Once homogenized, samples were centrifuged at 1200g for 10 minutes at 4°C. Total protein concentration of the supernatant was determined by Bradford assay (Bio-Rad Laboratories, CA, USA). All samples were diluted to a standard concentration of 1 $\mu g \cdot \mu l^{-1}$ with a Laemmli buffer containing β-mercaptoethanol. Samples were then denatured in boiling water for 5 minutes and immediately cooled in crushed ice for an additional 5 minutes. Proteins were separated using sodium dodecyl sulphate polyacrylamide gel electrophoresis (SDS-PAGE) on an 8-10% gradient gel for 90 minutes at 120V. Subsequently, the proteins were transferred on to either polyvinylidene fluoride (PVDF;

Millipore Bedford, MA, USA; IPVH00010; Pore size: 0.45μm) or nitrocellulose (Bio-Rad Laboratories, CA, USA; 162-0115; Pore size: 0.45μm) membranes at 100V for 90 minutes. Membranes were blocked in either BSA (bovine serum albumin) solution or milk-TBST (tris-buffered saline with 0.1% Tween-20; Sigma Aldrich, St Louis, MO, USA) solution at room temperature for 60 minutes. The membranes were then washed 5 times for 5 minutes each to ensure a low background and clean signal. Each membrane was cut just above 42 kDa and treated as two different membranes. The bottom half was used to blot for actin (the housekeeping protein used to normalize within membrane variance and the denominator when comparing treatment) and the top half was used to blot for the protein of interest. Primary antibodies were incubated (in various concentrations; see Appendix V) with either a 5% BSA or milk-TBST solution and agitated overnight at 4°C. Following another 5x5 minute wash, membranes were incubated in either an anti-rabbit or anti-mouse IgG horseradish peroxidase-conjugated secondary antibody (Cell Signaling, Danvers, MA USA; 7074) in room temperature for 60 minutes. Lastly, membranes were visualized by Chemiluminescent Substrate (Alpha Innotech, San Leandro, CA; 60-12596-00) and quantified using "*Image J*" software (National Institute of Mental Health, Bethesda, MD). Relative phophorylation was presented as a ratio of actin, and relative to ISO at 30 minutes for each membrane. Detailed Western Blotting Protocols can be found in appendix V.

6.6 Antibodies

Antibodies were purchased from the following sources (catalogue number in parenthesis): phospho-AMPK alpha (4188), Cell Signaling [Danvers, MA]; phospho-Akt [Thr^{208}] (2965), phospho-p44/42 MAPK [ERK1/2][Thr^{202}/Tyr^{204}](4370), Cell Signaling [Danvers, MA]; phospho-AS160 [pT^{642}] (33-1071G), Invitrogen/Biosource [Carlsbad, CA]; phospho-PKCα (06-822), Millipore [Billerica, MA] and anti-actin (612656), BD Transduction Laboratories [Franklin

Lakes, NJ]. Secondary anti-rabbit IGg, HRP-linked (7074) was also purchased from Cell Signaling [Danvers, MA]. Secondary anti-Mouse HRP-linked (A-4416) was purchased from Sigma Aldrich [St. Louis, MO].

6.7 Statistical Analysis

A two-way analysis of variance (ANOVA) was utilized to determine phosphorylation differences and metabolic concentrations. Osmotic condition (HYPER and ISO) and incubation times (30, 45 and 60 minutes) were treated as independent variables. If the two-way ANOVA showed any significance ($p<0.05$), a Tukey HSD post-hoc analysis was conducted to evaluate the significance of pair wise differences. All statistical analyses were conducted using SigmaStat 3.1 (Point Richmond, CA). All values are expressed as means ± standard deviations.

7. Results

7.1 General Observations

Rat weights and ages were not significantly different across all experimental groups.

Table 1: Average Rat Weights

Experimental Groups	Whole Rat Weight (g)	Rat Age (Days)
HYPER	131.1 ± 20.6	31.0 ± 3.8
ISO	130.2 ± 20.7	31.1 ± 3.7
NON	109.9 ± 8.4	27.2 ± 1.6

Note: All values are expressed as means ± SD. N =10 for HYPER and ISO groups. N=5 for NON group. HYPER = Hype-osmolality; ISO = Iso-osmolality; NON = non-incubated

7.2 Metabolites

PCr was significantly lower in HYPER compared to ISO group (main effect; Table 2). PCr in NON was not significantly different from ISO and HYPER. ATP concentrations within the EDL muscles were not different among any of the three groups.

Table 2: High Energy Phosphate Metabolite Concentrations

Conditions		[ATP]	[PCr]
ISO	30	28.50 ± 15.4	84.28 ± 30.0
	45	31.93 ± 4.6	107.87 ± 5.2
	60	32.57 ± 6.1	95.27 ± 28.2
HYPER†	30	31.09 ± 4.7	**52.75 ± 10.8**
	45	28.43 ± 4.2	**65.11 ± 6.4**
	60	29.81 ± 4.9	**86.64 ± 30.4**
NON		28.90 ± 4.3	77.04 ± 20.7

Note: All values are derived from random EDL samples from each condition and are expressed in mmol•kg^{-1} dry wt. (mean ± SD) N=3 for ISO and HYPER conditions. N=5 for NON conditions. ATP = adenosine triphosphate, PCr = phosphocreatine, ISO 30 = iso-osmotic condition incubated for 30 minutes. HYPER 30 = hyper-osmotic condition incubated for 30 minutes. NON = non-incubated controls. † Significantly different ($p<0.05$) from ISO (main effect). Bolding indicates the significance (†) corresponds with those values.

7.3 Time Course of Signaling Proteins

A preliminary pilot study was also conducted in our laboratory to investigate the time course of phosphorylation states during hyper-osmotic stimulation. The pilot study analyzed the phosphorylation states of Akt, AMPK, AS160 and ERK at 15, 30, 45 and 60 minutes of hyper-osmotic stress. Each lane was normalized to actin to control for loading variation. The results of this limited pilot study demonstrated that Akt and AMPK seemed to reach peak phosphorylation by 30 minutes, which was maintained through 45 minutes, and was followed by a rapid decline by 60 minutes (Figure 8). Correspondingly, ERK and AS160 phosphorylation increased drastically from 15 minutes and reached peak phosphorylation at 45 minutes (Figure 8). Interestingly, these pilot results suggested that Akt and AMPK may be involved near the proximal end of the cascade while ERK and AS160 are distal to Akt and AMPK. The results from this limited pilot study supported what was found in the literature, that phosphorylation differences should be detectable for all four proteins between 30 and 60 minutes of incubation with hyper-osmotic stress. Interestingly, previous work in our lab has also demonstrated significant increases in glucose uptake with hyper-osmotic stress during the same time frame (30 to 60 minutes) (unpublished thesis work) [19]. Therefore, for this study we chose to investigate the phosphorylation status of a number of signalling pathways potentially implicated in regulating glucose uptake in skeletal muscle.

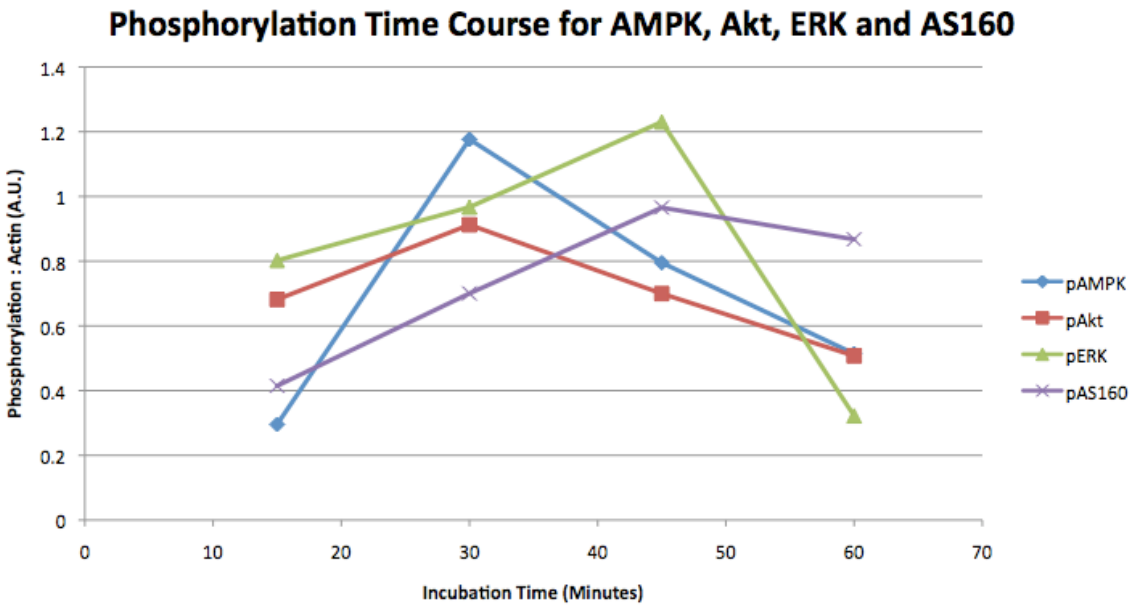

Figure 9: Results from a preliminary pilot study to determine an appropriate time course to detect differences in phosphorylation in AMPK, Akt, ERK, and AS160. AMPK = Adenosine monophosphate protein kinase, ERK = extracellular related kinase, AS160 = Akt substrate of 160kDa. N=1 per time point.

7.4 Signaling Proteins

AS160 showed a 1.7 fold increase in phosphorylation under HYPER stress when compared to ISO condition at 30 minutes ($p<0.01$, Figure 10). Interestingly, there was also a trend for a main effect for condition ($p=0.053$), such that there was an increase in phosphorylation for AS160 in HYPER as compared to ISO. A main effect for time was also revealed such that a decrease in phosphorylation was observed at 60 min compared to 45 min ($p<0.01$).

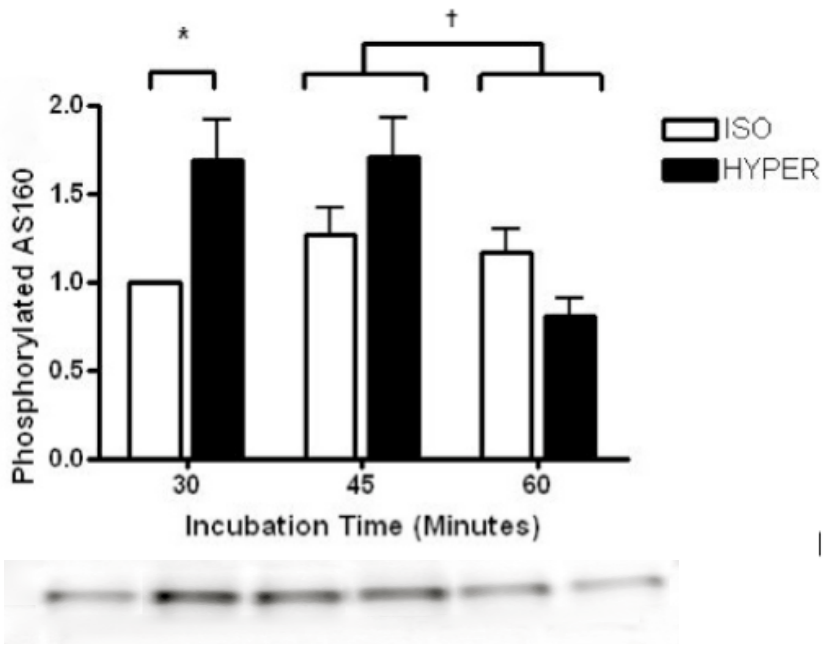

Figure 10: Phosphorylated AS160. Values are expressed as means ± SD. N=9-10 per condition. HYPER = Hyper-osmolality; ISO = Iso-osmolality. * Significant interaction difference ($p<0.01$). † Phosphorylation at 45 minutes was significantly higher than phosphorylation at 60 minutes (main effect; $p<0.01$)

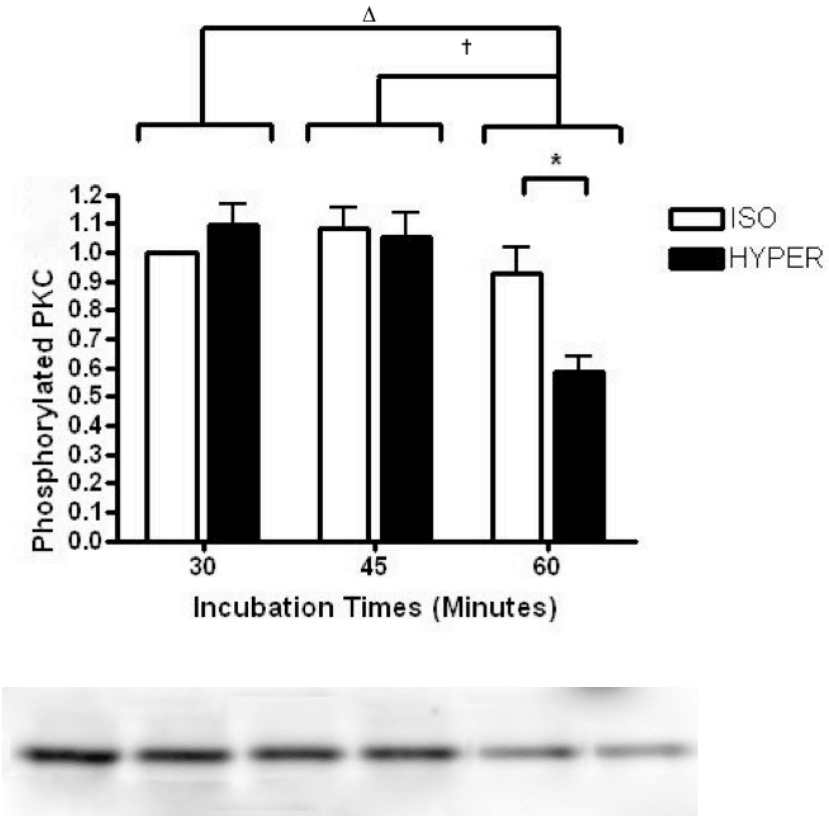

Figure 11: Phosphorylated PKCα. Values are expressed as means ± SD. N=9-10 per condition. HYPER = Hyper-osmolality; ISO = Iso-osmolality. * Significant interaction difference ($p<0.001$). Phosphorylation at 60 minutes was significantly lower than phosphorylation at 30 (Δ) and 45 minutes (†) ($p<0.001$)

Phosphorylation of cPKC was significantly lower in HYPER compared to ISO at 60 minutes of incubation ($p<0.01$, Figure 11). A significant main effect for time was also found for cPKC; phosphorylation at 30 minutes and 45 minutes were significantly higher than at 60 minutes ($p<0.001$).

No significant interactions were found for ERK phosphorylation across all time points and conditions (Figure 12). There was however, a significant main effect for time alone. Phosphorylation at 30 minutes was significantly higher than 45 minutes when condition was not considered ($p<0.05$).

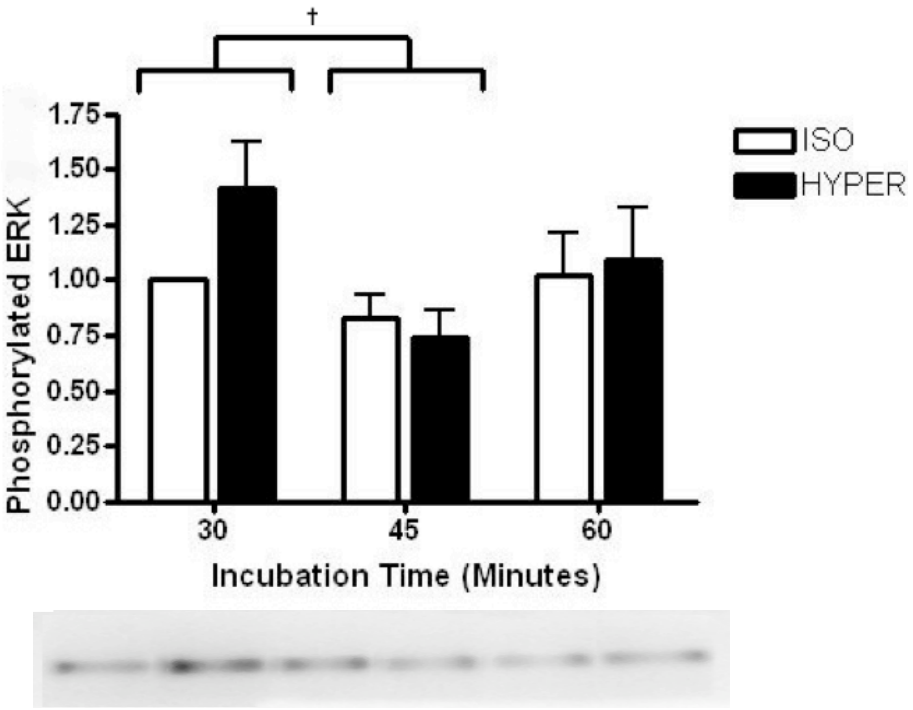

Figure 12: Phosphorylated ERK. Values are expressed as means ± SD. N=7-8 per condition. HYPER = Hyper-osmolality; ISO = Iso-osmolality. Phosphorylation at 30 minutes was significantly higher than phosphorylation at 45 minutes († main effect; $p<0.05$)

Akt phosphorylation (Figure 13) demonstrated a slight trend for a main effect for condition ($p=0.075$). Phosphorylation of HYPER trended higher than ISO when time was not considered. No differences were revealed for AMPK across all time points and conditions (Figure 14).

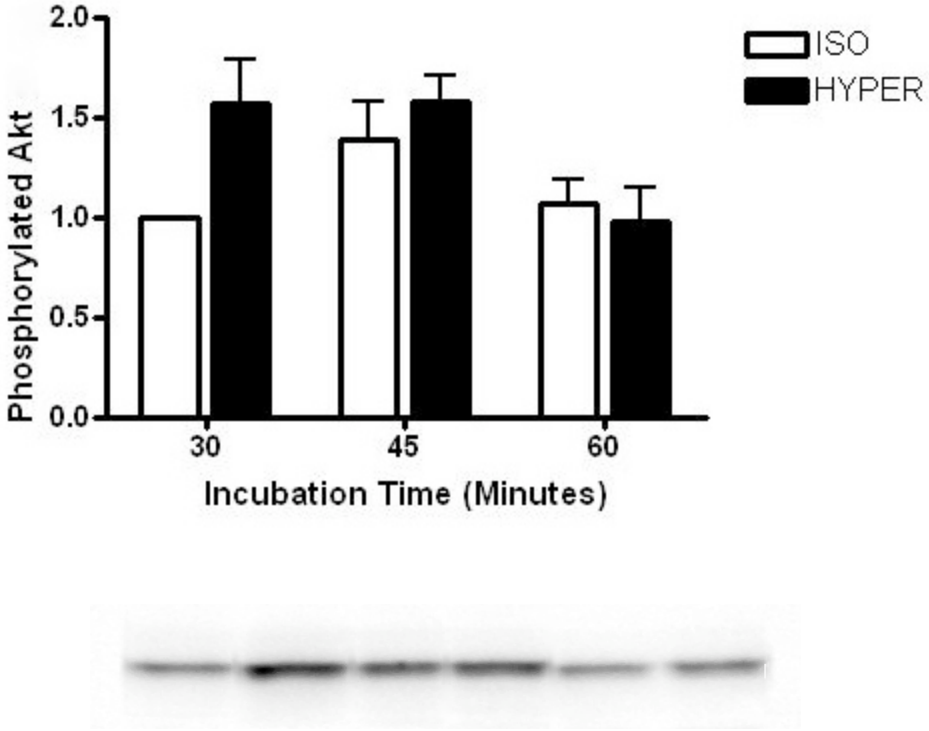

Figure 13: Phosphorylated Akt. Values are expressed as means ± SD. N=10 per condition. HYPER = Hyper-osmolality; ISO = Iso-osmolality.

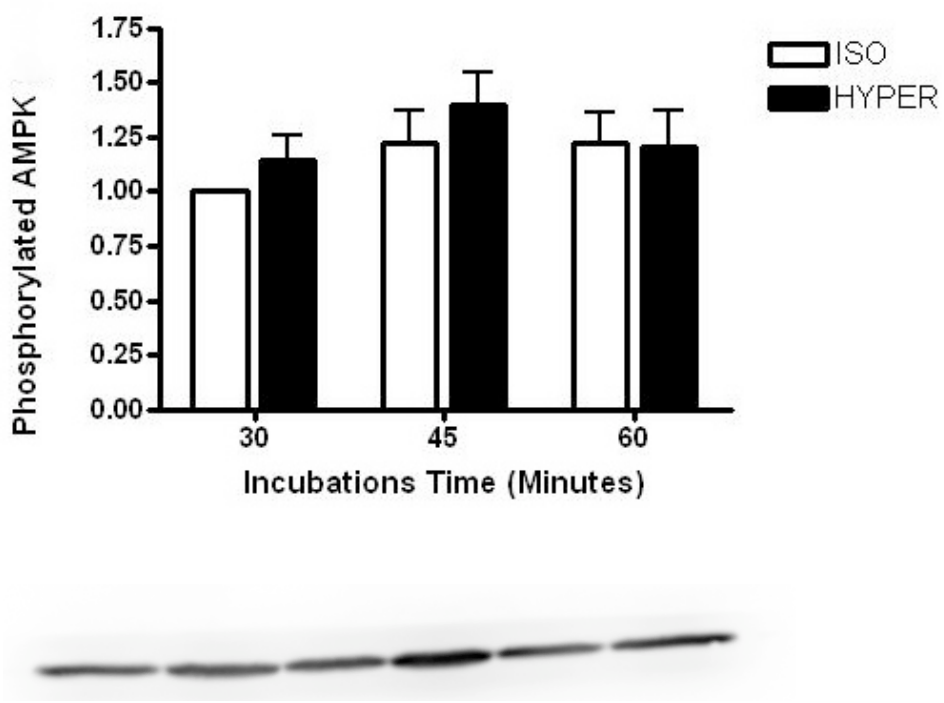

Figure 14: Phosphorylated AMPK. Values are expressed as means ± SD. N=7-8 per condition. HYPER = Hyper-osmolality; ISO = Iso-osmolality.

Lastly, expression of total Akt, AMPK, AS160 and ERK were determined in a pilot study (data not shown) conducted in our lab. Results demonstrated that total protein content did not change over the entire osmotic perturbation of 60 minutes for any of the proteins and any of the time points.

8. Discussion

The main finding of the current study was that AS160 phosphorylation was increased during the 30 and 60 minutes of hyper osmotic stress as compared to iso-osmotic conditions. Additionally, no changes in the phosphorylation states of; Akt, ERK, AMPK and cPKC were observed with hyper osmotic stress as compared to iso-osmotic control conditions. Finally, hyper-osmotic stress resulted in a significant decline in PCr, but no change in ATP.

8.1 Metabolites

Metabolites were measured in all the experimental groups to ensure the viability of the incubated muscles. Specifically, ATP and PCr content were measured from three random samples from each of ISO and HYPER groups, as well as five non-incubated (NON) muscles. Theoretically, the NON group represented the high energy phosphagen content of muscle in vivo, and the ISO group should have yielded a similar phosphagen content. In the current study, values were not significantly different between the NON and ISO groups, indicating the incubated muscles were viable and adequate oxygen diffused into the muscles during the incubations (Table 2). Furthermore, resting concentrations of ATP and PCr in skeletal muscle were ~25 mmol/kg and 79 mmol/kg of dry weight, respectively, and were similar to previously reported values obtained using a similar model [1, 57]. The NON and ISO groups in the current study matched the theoretical resting concentrations of both ATP and PCr. Lastly, PCr concentrations in the HYPER group were found to be significantly lower than the ISO group (Table 2). Such declines in PCr concentrations are common during HYPER, and have been attributed to increases in ATP turnover in response to the osmotic stress [2, 19, 51].

8.2 Glucose Signaling Summary

Figure 15 illustrates a hypothesized signaling scheme as a result of the current observations. AS160 is still hypothesized to be the convergence point for many stimulators and is directly responsible for GLUT4 translocation. It is encircled in a double oval, indicates that it is involved in osmotically stimulated glucose uptake after 30 minutes of stimulation. All the proteins encircled with a dashed oval, indicate that they appear not to be involved in osmotically stimulated glucose uptake after 30 minutes of hyper-osmotic stimulation in isolated muscle. Those proteins in a dotted oval indicate other possible proteins involved, but require further research.

The insulin signaling cascade is dependent on Akt, which was found to be inactive during hyper-osmotic stress after 30 minutes. Contraction is thought to stimulate glucose uptake through two mechanisms, energy depletion and calcium release. AMPK and ERK are involved in the energy depletion pathway and are not involved in osmotically stimulated glucose uptake between 30 and 60 minutes. cPKC may be involved in the calcium stimulated pathway and results show that it may not be involved with osmotically stimulated glucose uptake after 30 minutes of hyper-osmotic stress. Hyper-osmotic stress seems to phosphorylate AS160 similar to insulin and contraction. During insulin and contraction stimulated glucose uptake, AS160 is phosphorylated between 30 and 60 minutes under the appropriate stimulation [9, 74]. This may indicate that the signaling mechanisms of the three stimulators begin on divergent pathways, but eventually converge to the same point. Further research is required to explore other proteins actively involved in signaling glucose uptake under hyper-osmotic stress. In addition, further research is required to clarify the signaling related events involving Akt, AMPK, ERK, cPKC and AS160 prior to 30 minutes of incubation of skeletal muscle in a hyper-osmotic environment.

8.3 AS160

The most important finding of the current investigation was that phosphorylation of AS160 was significantly higher in the HYPER condition compared to the ISO condition at 30 minutes. Recall that phosphorylation of AS160 transforms AS160 to become less active therefore releasing the inhibition on downstream Rab targets ultimately leading to increase GLUT4 translocation and glucose uptake. Therefore the current finding advances the possibility that AS160 may be a key signaling protein in osmotically induced glucose uptake.

Thong et al. in 2007 have been the only group to date that has investigated AS160 phosphorylation with hyper-osmotic stress and mixed results were reported [76]. Thong reported that in CHO-IR cell culture, but not L6 muscle cell culture, that AS160 phosphorylation was required for osmotically induced glucose uptake [76]. Results from the present study suggest that AS160 is phosphorylated under hyper-osmotic stress in whole skeletal muscle and may contribute to the increase in glucose uptake.

It is worthy to note that AS160 is hypothesized to be one of the last proteins involved in the osmotic signaling cascade. Somewhere between 30 minutes and 45 minutes, phosphorylation seems to return to basal levels. The pilot study mentioned above, suggested that AS160 phosphorylation reaches phosphorylation at 45 minutes, and more importantly, after Akt and AMPK. The current data does not rule out other possible signaling cascades that could also influence AS160. Future work should focus on determining how rapidly phosphorylation of AS160 occurs and if varying degrees of osmotic stress alter this response.

8.4 cPKC

Our cPKC data suggests two possible situations, one being that peak phosphorylation states occur before 30 minutes (Figure 11), or that cPKC is not involved. At 60 minutes,

phosphorylation was significantly lower in HYPER compared to ISO. The reason for this phenomenon is unknown. cPKC was included in this investigation to evaluate the hypothesis that calcium sparks may provide a signal that contributes to the increases in glucose uptake [68] that are observed with osmotic stress. Calcium sparks are transient events and the peak of cPKC phosphorylation may have occurred prior to our earliest time point, therefore eluding our ability to detect cPKC phosphorylation. In fact, research by Bartlett et al. has suggested that cPKC responses mimic the oscillatory patterns of calcium [8], and if this is true, phosphorylation of cPKC could be intermittent or transitory. Lastly, cPKCα is only one isoform of the conventional PKCs, and perhaps other isoforms such as the β and/or γ isoforms work in concert with PKCα to produce a more substantial signal. In addition, the PKC family is regulated by many spatial factors, such as DAGs and heat shock proteins, and as such, phosphorylation of the protein may not tell the full story of its true activity [26]. Therefore, a more in-depth examination of other PKC isoforms and other regulatory factors is necessary to better understand the possible role of PKC in osmotically induced glucose uptake.

8.5 AMPK

In the current study, no difference in phosphorylation of AMPK was observed between conditions across all time points (Figure 14), even despite a decline in PCr as expected in HYPER. The role of AMPK in osmotically induced glucose uptake in both muscle cell culture [32, 54, 76] and adipose cell culture [21] has been previously been investigated; however results have been very inconclusive. Fryer suggested that AMPK is essential for hyper-osmotic induced glucose uptake in C1C12 cell culture [21, 32]. Similarly, Hayashi reported AMPK was also essential for sorbitol induced glucose uptake in isolated rat epitrochlearis muscle [32]. However, Patel and Thong have independently reported that AMPK was not required for glucose uptake under hyper-osmotic stress in L6 muscle culture [54, 76]. In addition, Fujii et al. used an AMPK knock

out (KO) mouse model to investigate AMPK's role in glucose uptake [23] and found AMPK was not essential for glucose transport. Fujii and Hayashi have been the only two groups to use whole skeletal muscle, however their results require clarification due to conflicting results and the KO model used. Research involving KO animals always carries the possibility of unknown/unwanted side effects or compensations in physiological function and control.

The current study provides support to the observations of Patel and Thong's, where they observed that AMPK was not involved in osmotically induced glucose uptake in whole skeletal muscle under physiological hyper osmotic stress after 30 minutes. These results contrast both Fryer and Hayashi findings [21, 22, 32]. Differences from Fryer's results could be attributed to the differences in models used, as characteristics between whole skeletal muscle and C1C12 cell culture are not always consistent. Furthermore, Hayashi's observations might be partially related to the fuel status of their sorbitol-treated cells in culture. Hayashi reported intramuscular concentrations of ATP, PCr and glycogen that were significantly lower with the sorbitol treated cells as compared to control cells [32], suggesting a more marked energy compromise. In contrast, in the current study and other studies previously done in our laboratory, ATP concentrations were maintained across all conditions [19, 51]. The osmolality of the HYPER condition in the current study (400 mmol/kg) was specifically chosen to mimic physiological osmolalities seen during high intensity exercise [46]. Hayashi's perturbation of 120mmol/L of sorbitol was measured in our lab using the VAPRO pressure osmometer (VAPRO5520, Westcor, Logan, UT), and resulted in an average osmolality of 123 mmol/kg, which is considered hypo-osmotic under normal physiological conditions. All in all, the drop in ATP and hypo rather than hyper-osmotic environment demonstrates a non-viable and/or drastically different incubation protocol that likely contributed to the disparate AMPK activation. Further

work is required to better understand the role of AMPK in osmotically stimulated glucose uptake.

8.6 ERK

Data from the current study found no differences in ERK phosphorylation between ISO and HYPER conditions after 30 minutes of incubation. This is in contrast to the observations of Sajan et al., who found increased ERK phosphorylation during the first 30 minutes of osmotic stress. It is possible that the ERK signal was much more active before 30 minutes compared to after 30 minutes during the current study. ERK has been previously hypothesized to be involved in osmotically stimulated glucose uptake downstream of PYK2 in both rat adipocyte and L6 muscle cell culture [65]. Sajan et al. used inhibitors in the various tissue models to determine aPKCs were activated downstream of a RAS/RAF/MEK1/PYK2/ERK-dependant pathway [65]. The observed differences could also be attributed to the different models used, cell culture vs. isolated muscle.

Chen et al. has previously reported ERK to be activated downstream of AMPK during "exercise" in both mouse EDL and L6 myotubes [12]. The "exercise" effect was achieved by artificially stimulating AMPK using AICAR. Increased glucose uptake and activation of ERK and aPKCs were observed with AICAR stimulation. However, in the current study AMPK was found to be inactive between 30 and 60 minutes of incubation, it is not surprising that ERK was also found to be inactive between 30 and 60 minutes based on the reported relationship of these two signals. Conversely, ERK was also hypothesized to be phosphorylated around the same time point as AS160, if not slightly earlier.

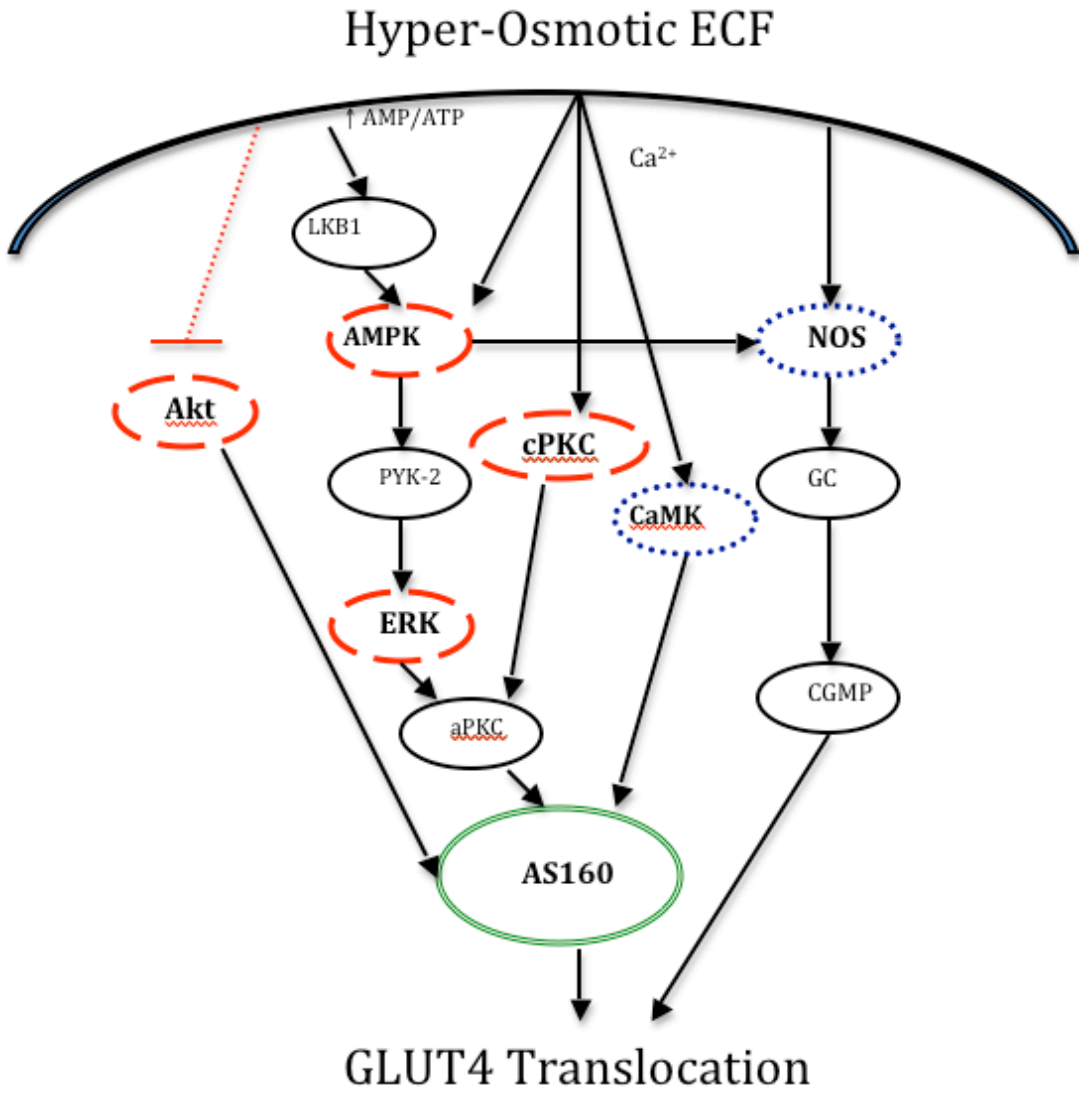

Figure 15: Mechanism for hyper-osmotic glucose uptake. Proteins within a double oval (AS160) may be involved in hyper-osmotic glucose uptake between 30 and 60 minutes. Proteins encircled in a dashed oval are not involved with hyper-osmotic glucose uptake between 30 and 60 minutes of hyper-osmotic stress. Proteins encircled by a dotted oval are other proteins that have not been studied in this investigation but warrant further research to clarify their role in hyper-osmotic glucose uptake.

8.7 Akt

Akt is considered the centerpiece of the insulin signaling cascade. It is thought to be directly upstream of AS160 and its activation would provide evidence of any upstream activation of the insulin signaling cascade. Signaling proteins such as PI3-K and PDK are associated with many different signaling pathways and lead to Akt activation. The findings of the current study supported the original hypothesis that Akt phosphorylation would be similar between ISO and HYPER conditions at all time points. Recall that osmotic stress was thought to inhibit insulin signaling via inhibition of Akt phosphorylation. Therefore, it appears unlikely that upstream kinases like PI3-K and PDK are involved in osmotically stimulated glucose uptake between 30 and 60 minutes of hyper osmotic incubation.

8.8 Conclusions

In summary, an increase in AS160 phosphorylation was observed between 30 and 60 minutes of incubation as compared to iso-osmotic conditions. Furthermore, no changes in the phosphorylation states of; Akt, ERK, AMPK and cPKC were observed with hyper osmotic stress as compared to iso-osmotic control conditions. This suggests that AS160 is involved in osmotically stimulated glucose uptake following 30 minutes of osmotic stimulation. On the contrary, Akt, a major signal in the insulin stimulated pathway does not appear to be involved with such stimulation. Furthermore, the phosphorylation state of signaling pathways originally described to be involved in contraction stimulated or stress related activation of glucose uptake (AMPK, ERK and cPKC) remained similar between hyper-osmotic and iso-osmotic conditions from 30 to 60 minutes of incubation. Future research should attempt to fully elucidate the time frame of activation (phosphorylation) of the pathways implicated in glucose uptake, especially from 0 to 30 minutes of stimulation, to develop a full understanding of the mechanisms underlying hyper-osmotic stress induced glucose uptake.

8.9 Future Directions

Glucose regulation is an extremely complex and very important system within skeletal muscle. It is well established that redundant signaling pathways exist and that many more proteins are involved than the few studied here. In fact, most of the proteins characterized in this study do not appear to be involved in osmotically stimulated glucose uptake between 30 and 60 minutes of stimulation. Thus, an obvious next step is to continue to profile the likely signaling candidates that may be involved. As mentioned earlier, CaMK is another protein that should be investigated to explore the possibility that calcium maybe a key secondary messenger in regards to glucose uptake under such conditions. To the authors knowledge, no literature has investigated the interaction of osmotic stress and CaMK, however, a number of articles do exist that demonstrate a link between contraction stimulated glucose uptake and CaMK [35, 86]. There is also growing evidence demonstrating the osmotic stress leads to intermittent calcium release through the DHPR of the sarcoplasmic reticulum (REFS). Such increases in calcium could lead to CaMK activation and may provide a link to activation of glucose uptake.

Nitric oxide synthase (NOS) is another signaling protein that may be involved in osmotically stimulated glucose uptake. Traditionally, NOS is thought to be phosphorylated downstream of AMPK and regulate GLUT4 translocation through increased guanylate cyclase activity (GC) [22, 28]. However, we did not observe an increase in AMPK activation following 30 minutes of hyper-osmotic stress, however, there hav been suggestions that NOS might be regulated independently of AMPK [49]. Therefore, future work should investigate if it is possible for NOS to regulate osmotically induced glucose uptake independent of AMPK.

In addition to exploring other proteins in the osmotic signaling cascade, it would be very valuable to fully establish the time frame for signaling of the various pathways throughout a

period of osmotic stress. Recommended time points for a follow-up experiment should include 5, 15 and 30 minutes of incubations in both ISO and HYPER conditions.

Lastly, it would be interesting to consider other aspects of GLUT4 translocation, that is, GLUT4 internalization and GLUT4 activation. The vast majority of research has focused on the exocytotic portion of glucose uptake, however osmotically stimulated glucose uptake may be achieved through a decrease rate in GLUT4 internalization. It would be worth researching proteins involved with GLUT4 internalization, such as clathrin, transferrin receptors, SNARES, VAMPs and other adaptor proteins. GLUT4 activation should also be considered as GLUT4 surface content does not necessarily imply that glucose is taken up.

REFERENCES

1. Angeras, U., M. Hall-Angeras, K.R. Wagner, H. James, P.O. Hasselgren, and J.E. Fischer, *Tissue metabolite levels in different types of skeletal muscle during sepsis.* Metabolism, 1991. **40**(11): p. 1147-51.

2. Antolic, A., R. Harrison, C. Farlinger, N.M. Cermak, S.J. Peters, P. LeBlanc, and B.D. Roy, *Effect of extracellular osmolality on cell volume and resting metabolism in mammalian skeletal muscle.* Am J Physiol Regul Integr Comp Physiol 2007. **292**(5): p. R1994-2000.

3. Antonescu, C.N., M. Diaz, G. Femia, J.V. Planas, and A. Klip, *Clathrin-dependent and independent endocytosis of glucose transporter 4 (GLUT4) in myoblasts: regulation by mitochondrial uncoupling.* Traffic, 2008. **9**(7): p. 1173-90.

4. Antonescu, C.N., M. Foti, N. Sauvonnet, and A. Klip, *Ready, set, internalize: mechanisms and regulation of GLUT4 endocytosis.* Biosci Rep, 2009. **29**(1): p. 1-11.

5. Apostol, S., D. Ursu, F. Lehmann-Horn, and W. Melzer, *Local calcium signals induced by hyper-osmotic stress in mammalian skeletal muscle cells.* J Muscle Res Cell Motil, 2009. **30**(3-4): p. 97-109.

6. Barac-Nieto, M., G.B. Spurr, H. Lotero, M.G. Maksud, and H.W. Dahners, *Body composition during nutritional repletion of severely undernourished men.* Am J Clin Nutr, 1979. **32**(5): p. 981-91.

7. Baron, A.D., G. Brechtel, P. Wallace, and S.V. Edelman, *Rates and tissue sites of non-insulin- and insulin-mediated glucose uptake in humans.* Am J Physiol, 1988. **255**(6 Pt 1): p. E769-74.

8. Bartlett, P.J., K.W. Young, S.R. Nahorski, and R.A. Challiss, *Single cell analysis and temporal profiling of agonist-mediated inositol 1,4,5-trisphosphate, Ca2+, diacylglycerol, and protein kinase C signaling using fluorescent biosensors.* J Biol Chem, 2005. **280**(23): p. 21837-46.

9. Bruss, M.D., E.B. Arias, G.E. Lienhard, and G.D. Cartee, *Increased phosphorylation of Akt substrate of 160 kDa (AS160) in rat skeletal muscle in response to insulin or contractile activity.* Diabetes, 2005. **54**(1): p. 41-50.

10. Carmena, D. and A. Sardini, *Lifespan regulation of conventional protein kinase C isotypes.* Biochem Soc Trans, 2007. **35**(Pt 5): p. 1043-5.

11. Chen, D., R.V. Fucini, A.L. Olson, B.A. Hemmings, and J.E. Pessin, *Osmotic shock inhibits insulin signaling by maintaining Akt/protein kinase B in an inactive dephosphorylated state.* Mol Cell Biol, 1999. **19**(7): p. 4684-94.

12. Chen, H.C., G. Bandyopadhyay, M.P. Sajan, Y. Kanoh, M. Standaert, R.V. Farese, Jr., and R.V. Farese, *Activation of the ERK pathway and atypical protein kinase C isoforms in exercise- and aminoimidazole-4-carboxamide-1-beta-D-riboside (AICAR)-stimulated glucose transport.* J Biol Chem, 2002. **277**(26): p. 23554-62.

13. Chen, S., J. Murphy, R. Toth, D.G. Campbell, N.A. Morrice, and C. Mackintosh, *Complementary regulation of TBC1D1 and AS160 by growth factors, insulin and AMPK activators.* Biochem J, 2008. **409**(2): p. 449-59.

14. Close, R., *Dynamic Properties of Fast and Slow Skeletal Muscles of the Rat during Development.* J Physiol, 1964. **173**: p. 74-95.

15. Costill, D.L., R. Cote, and W. Fink, *Muscle water and electrolytes following varied levels of dehydration in man.* J Appl Physiol, 1976. **40**(1): p. 6-11.

16. Deshmukh, A., V.G. Coffey, Z. Zhong, A.V. Chibalin, J.A. Hawley, and J.R. Zierath, *Exercise-induced phosphorylation of the novel Akt substrates AS160 and filamin A in human skeletal muscle.* Diabetes, 2006. **55**(6): p. 1776-82.

17. Deshmukh, A.S., J.A. Hawley, and J.R. Zierath, *Exercise-induced phospho-proteins in skeletal muscle.* Int J Obes (Lond), 2008. **32 Suppl 4**: p. S18-23.

18. Dugani, C.B. and A. Klip, *Glucose transporter 4: cycling, compartments and controversies.* EMBO Rep, 2005. **6**(12): p. 1137-42.

19. Farlinger, C., *The Influence of Skeletal Muscle Cell Volume on the Regulation of Carbohydrate Uptake and Muscle Metabolism*, in *Faculty of Applied Health Sciences*. 2007, Brock University: St. Catharines, Ontario.

20. Foster, L.J., D. Li, V.K. Randhawa, and A. Klip, *Insulin accelerates inter-endosomal GLUT4 traffic via phosphatidylinositol 3-kinase and protein kinase B.* J Biol Chem, 2001. **276**(47): p. 44212-21.

21. Fryer, L.G., F. Foufelle, K. Barnes, S.A. Baldwin, A. Woods, and D. Carling, *Characterization of the role of the AMP-activated protein kinase in the stimulation of glucose transport in skeletal muscle cells.* Biochem J 2002. **363**(Pt 1): p. 167-74.

22. Fryer, L.G., E. Hajduch, F. Rencurel, I.P. Salt, H.S. Hundal, D.G. Hardie, and D. Carling, *Activation of glucose transport by AMP-activated protein kinase via stimulation of nitric oxide synthase.* Diabetes, 2000. **49**(12): p. 1978-85.

23. Fujii, N., M.F. Hirshman, E.M. Kane, R.C. Ho, L.E. Peter, M.M. Seifert, and L.J. Goodyear, *AMP-activated protein kinase alpha2 activity is not essential for contraction- and hyperosmolarity-induced glucose transport in skeletal muscle.* J Biol Chem, 2005. **280**(47): p. 39033-41.

24. Gisolfi, C.V. and D.R. Lamb, *Fluid Homeostasis During Exercise* Perspectives in Exercise Science and Sports Medicine. 2001, Traverse City, MI, USA: Cooper Publishing Group.

25. Gosmanov, A.R., E.G. Schneider, and D.B. Thomason, *NKCC activity restores muscle water during hyperosmotic challenge independent of insulin, ERK, and p38 MAPK.* Am J Physiol Regul Integr Comp Physiol, 2003. **284**(3): p. R655-65.

26. Gould, C.M. and A.C. Newton, *The life and death of protein kinase C.* Curr Drug Targets, 2008. **9**(8): p. 614-25.

27. Green, H.J., J.A. Thomson, and M.E. Houston, *Supramaximal exercise after training-induced hypervolemia. II. Blood/muscle substrates and metabolites.* J Appl Physiol, 1987. **62**(5): p. 1954-61.

28. Gual, P., Y. Le Marchand-Brustel, and J. Tanti, *Positive and negative regulation of glucose uptake by hyperosmotic stress.* Diabetes Metab, 2003. **29**(6): p. 566-75.

29. Hansen, S.H., K. Sandvig, and B. van Deurs, *Clathrin and HA2 adaptors: effects of potassium depletion, hypertonic medium, and cytosol acidification.* J Cell Biol, 1993. **121**(1): p. 61-72.

30. Harris, R.C., E. Hultman, and L.O. Nordesjo, *Glycogen, glycolytic intermediates and high-energy phosphates determined in biopsy samples of musculus quadriceps femoris of man at rest. Methods and variance of values.* Scand J Clin Lab Invest, 1974. **33**(2): p. 109-20.

31. Haussinger, D., F. Lang, and W. Gerok, *Regulation of cell function by the cellular hydration state.* Am J Physiol, 1994. **267**(3 Pt 1): p. E343-55.

32. Hayashi, T., M.F. Hirshman, N. Fujii, S.A. Habinowski, L.A. Witters, and L.J. Goodyear, *Metabolic stress and altered glucose transport: activation of AMP-activated protein kinase as a unifying coupling mechanism.* Diabetes, 2000. **49**(4): p. 527-31.

33. Huang, S. and M.P. Czech, *The GLUT4 glucose transporter.* Cell Metab, 2007. **5**(4): p. 237-52.

34. Ishiki, M. and A. Klip, *Minireview: recent developments in the regulation of glucose transporter-4 traffic: new signals, locations, and partners.* Endocrinology, 2005. **146**(12): p. 5071-8.

35. Jensen, T.E., A.J. Rose, S.B. Jorgensen, N. Brandt, P. Schjerling, J.F. Wojtaszewski, and E.A. Richter, *Possible CaMKK-dependent regulation of AMPK phosphorylation and glucose uptake at the onset of mild tetanic skeletal muscle contraction.* Am J Physiol Endocrinol Metab, 2007. **292**(5): p. E1308-17.

36. Jessen, N. and L.J. Goodyear, *Contraction signaling to glucose transport in skeletal muscle.* J Appl Physiol Category Category, 2005. **99**(1): p. 330-7.

37. Kane, S., H. Sano, S.C. Liu, J.M. Asara, W.S. Lane, C.C. Garner, and G.E. Lienhard, *A method to identify serine kinase substrates. Akt phosphorylates a novel adipocyte protein with a Rab GTPase-activating protein (GAP) domain.* J Biol Chem, 2002. **277**(25): p. 22115-8.

38. Khayat, Z.A., T. Tsakiridis, A. Ueyama, R. Somwar, Y. Ebina, and A. Klip, *Rapid stimulation of glucose transport by mitochondrial uncoupling depends in part on cytosolic Ca2+ and cPKC.* Am J Physiol, 1998. **275**(6 Pt 1): p. C1487-97.

39. Klip, A., *The many ways to regulate glucose transporter 4.* Appl Physiol Nutr Metab, 2009. **34**(3): p. 481-7.

40. Kraft, P.A., *The osmotic shift.* J Intraven Nurs, 2000. **23**(4): p. 220-4.

41. Kramer, H.F., E.B. Taylor, C.A. Witczak, N. Fujii, M.F. Hirshman, and L.J. Goodyear, *Calmodulin-binding domain of AS160 regulates contraction- but not insulin-stimulated glucose uptake in skeletal muscle.* Diabetes 2007. **56**(12): p. 2854-62.

42. Lang, F., *Mechanisms and significance of cell volume regulation.* J Am Coll Nutr, 2007. **26**(5 Suppl): p. 613S-623S.

43. Lang, F., G.L. Busch, M. Ritter, H. Volkl, S. Waldegger, E. Gulbins, and D. Haussinger, *Functional significance of cell volume regulatory mechanisms.* Physiol Rev, 1998. **78**(1): p. 247-306.

44. Leng, Y., T.L. Steiler, and J.R. Zierath, *Effects of insulin, contraction, and phorbol esters on mitogen-activated protein kinase signaling in skeletal muscle from lean and ob/ob mice.* Diabetes, 2004. **53**(6): p. 1436-44.

45. Li, D., V.K. Randhawa, N. Patel, M. Hayashi, and A. Klip, *Hyperosmolarity reduces GLUT4 endocytosis and increases its exocytosis from a VAMP2-independent pool in l6 muscle cells.* J Biol Chem, 2001. **276**(25): p. 22883-91.

46. Lindinger, M.I., T.J. Hawke, S.L. Lipskie, H.D. Schaefer, and L. Vickery, *K(+) transport and volume regulatory response by NKCC in resting rat hindlimb skeletal muscle.* Cell Physiol Biochem, 2002. **12**(5-6): p. 279-92.

47. Maxfield, F.R. and T.E. McGraw, *Endocytic recycling.* Nat Rev Mol Cell Biol, 2004. **5**(2): p. 121-32.

48. McConell, G.K. and G.D. Wadley, *Potential role of nitric oxide in contraction-stimulated glucose uptake and mitochondrial biogenesis in skeletal muscle.* Clin Exp Pharmacol Physiol, 2008. **35**(12): p. 1488-92.

49. Merry, T.L., G.R. Steinberg, G.S. Lynch, and G.K. McConell, *Skeletal muscle glucose uptake during contraction is regulated by nitric oxide and ROS independently of AMPK.* Am J Physiol Endocrinol Metab. **298**(3): p. E577-85.

50. Michelle Furtado, L., V. Poon, and A. Klip, *GLUT4 activation: thoughts on possible mechanisms.* Acta Physiol Scand Category Category, 2003. **178**(4): p. 287-96.

51. Mulligan, M.J., *Glucose Dynamics in Rat Skeletal Muscle: Recovery From Osmotic Stress*, in *Faculty of Applied Health Studies*. 2008, Brock University: St Catharines.

52. Musi, N. and L.J. Goodyear, *AMP-activated protein kinase and muscle glucose uptake.* Acta Physiol Scand, 2003. **178**(4): p. 337-45.

53. Okada, Y., *Ion channels and transporters involved in cell volume regulation and sensor mechanisms.* Cell Biochem Biophys, 2004. **41**(2): p. 233-58.

54. Patel, N., Z.A. Khayat, N.B. Ruderman, and A. Klip, *Dissociation of 5' AMP-activated protein kinase activation and glucose uptake stimulation by mitochondrial uncoupling and hyperosmolar stress: differential sensitivities to intracellular Ca2+ and protein kinase C inhibition.* Biochem Biophys Res Commun 2001. **285**(4): p. 1066-70.

55. Pessin, J.E. and A.R. Saltiel, *Signaling pathways in insulin action: molecular targets of insulin resistance.* J Clin Invest, 2000. **106**(2): p. 165-9.

56. Ploug, T., H. Galbo, J. Vinten, M. Jorgensen, and E.A. Richter, *Kinetics of glucose transport in rat muscle: effects of insulin and contractions.* Am J Physiol, 1987. **253**(1 Pt 1): p. E12-20.

57. Poortmans, J.R., *Principles of Exercise Biochemistry*. 3rd ed. Medicine and Sport Science, ed. M.H.B. J. Borms (Brussels), A.P. Hills (Brisbane). Vol. 46. 2004, Brussels, Belgium Karger

58. Proctor, D.N., P.C. O'Brien, E.J. Atkinson, and K.S. Nair, *Comparison of techniques to estimate total body skeletal muscle mass in people of different age groups.* Am J Physiol, 1999. **277**(3 Pt 1): p. E489-95.

59. Ramm, G., M. Larance, M. Guilhaus, and D.E. James, *A role for 14-3-3 in insulin-stimulated GLUT4 translocation through its interaction with the RabGAP AS160.* J Biol Chem, 2006. **281**(39): p. 29174-80.

60. Randhawa, V.K., F.S. Thong, D.Y. Lim, D. Li, R.R. Garg, R. Rudge, T. Galli, A. Rudich, and A. Klip, *Insulin and hypertonicity recruit GLUT4 to the plasma membrane of muscle cells by using N-ethylmaleimide-sensitive factor-dependent SNARE mechanisms but different v-SNAREs: role of TI-VAMP.* Mol Biol Cell, 2004. **15**(12): p. 5565-73.

61. Ritz, P. and G. Berrut, *The importance of good hydration for day-to-day health.* Nutr Rev, 2005. **63**(6 Pt 2): p. S6-13.

62. Ritz, P., A. Salle, G. Simard, J.F. Dumas, F. Foussard, and Y. Malthiery, *Effects of changes in water compartments on physiology and metabolism.* Eur J Clin Nutr 2003. **57 Suppl 2**: p. S2-5.

63. Roux, P.P. and J. Blenis, *ERK and p38 MAPK-activated protein kinases: a family of protein kinases with diverse biological functions.* Microbiol Mol Biol Rev Category Category, 2004. **68**(2): p. 320-44.

64. Rudich, A. and A. Klip, *Push/pull mechanisms of GLUT4 traffic in muscle cells.* Acta Physiol Scand Category Category, 2003. **178**(4): p. 297-308.

65. Sajan, M.P., G. Bandyopadhyay, Y. Kanoh, M.L. Standaert, M.J. Quon, B.C. Reed, I. Dikic, and R.V. Farese, *Sorbitol activates atypical protein kinase C and GLUT4 glucose transporter translocation/glucose transport through proline-rich tyrosine kinase-2, the extracellular signal-regulated kinase pathway and phospholipase D.* Biochem J Category Category, 2002. **362**(Pt 3): p. 665-74.

66. Sakamoto, K. and G.D. Holman, *Emerging role for AS160/TBC1D4 and TBC1D1 in the regulation of GLUT4 traffic.* Am J Physiol Endocrinol Metab 2008. **295**(1): p. E29-37.

67. Sano, H., S. Kane, E. Sano, C.P. Miinea, J.M. Asara, W.S. Lane, C.W. Garner, and G.E. Lienhard, *Insulin-stimulated phosphorylation of a Rab GTPase-activating protein regulates GLUT4 translocation.* J Biol Chem, 2003. **278**(17): p. 14599-602.

68. Santos, J.M., S.B. Ribeiro, A.R. Gaya, H.J. Appell, and J.A. Duarte, *Skeletal muscle pathways of contraction-enhanced glucose uptake.* Int J Sports Med Category Category, 2008. **29**(10): p. 785-94.

69. Sawka, M.N., S.N. Cheuvront, and R. Carter, 3rd, *Human water needs.* Nutr Rev 2005. **63**(6 Pt 2): p. S30-9.

70. Sawka, M.N. and S.J. Montain, *Fluid and electrolyte supplementation for exercise heat stress.* Am J Clin Nutr, 2000. **72**(2 Suppl): p. 564S-72S.

71. Shaw, R.J., M. Kosmatka, N. Bardeesy, R.L. Hurley, L.A. Witters, R.A. DePinho, and L.C. Cantley, *The tumor suppressor LKB1 kinase directly activates AMP-activated kinase and regulates apoptosis in response to energy stress.* Proc Natl Acad Sci U S A, 2004. **101**(10): p. 3329-35.

72. Silverthorn, D.U., *Human Physiology*. 4th ed. 2007, San Francisco, CA: Pearson Education, Inc.

73. Somwar, R., D.Y. Kim, G. Sweeney, C. Huang, W. Niu, C. Lador, T. Ramlal, and A. Klip, *GLUT4 translocation precedes the stimulation of glucose uptake by insulin in muscle*

cells: potential activation of GLUT4 via p38 mitogen-activated protein kinase. Biochem J, 2001. **359**(Pt 3): p. 639-49.

74. Sriwijitkamol, A., D.K. Coletta, E. Wajcberg, G.B. Balbontin, S.M. Reyna, J. Barrientes, P.A. Eagan, C.P. Jenkinson, E. Cersosimo, R.A. DeFronzo, K. Sakamoto, and N. Musi, *Effect of acute exercise on AMPK signaling in skeletal muscle of subjects with type 2 diabetes: a time-course and dose-response study.* Diabetes, 2007. **56**(3): p. 836-48.

75. Strange, K., *Cellular volume homeostasis.* Adv Physiol Educ, 2004. **28**(1-4): p. 155-9.

76. Thong, F.S., P.J. Bilan, and A. Klip, *The Rab GTPase-activating protein AS160 integrates Akt, protein kinase C, and AMP-activated protein kinase signals regulating GLUT4 traffic.* Diabetes, 2007. **56**(2): p. 414-23.

77. Thong, F.S., C.B. Dugani, and A. Klip, *Turning signals on and off: GLUT4 traffic in the insulin-signaling highway.* Physiology (Bethesda), 2005. **20**: p. 271-84.

78. Treebak, J.T. and J.F. Wojtaszewski, *Role of 5'AMP-activated protein kinase in skeletal muscle.* Int J Obes (Lond), 2008. **32 Suppl 4**: p. S13-7.

79. Von Duvillard, S.P., W.A. Braun, M. Markofski, R. Beneke, and R. Leithauser, *Fluids and hydration in prolonged endurance performance.* Nutrition, 2004. **20**(7-8): p. 651-6.

80. Wang, Q., R. Somwar, P.J. Bilan, Z. Liu, J. Jin, J.R. Woodgett, and A. Klip, *Protein kinase B/Akt participates in GLUT4 translocation by insulin in L6 myoblasts.* Mol Cell Biol, 1999. **19**(6): p. 4008-18.

81. Wang, X., N. Weisleder, C. Collet, J. Zhou, Y. Chu, Y. Hirata, X. Zhao, Z. Pan, M. Brotto, H. Cheng, and J. Ma, *Uncontrolled calcium sparks act as a dystrophic signal for mammalian skeletal muscle.* Nat Cell Biol, 2005. **7**(5): p. 525-30.

82. Wasserman, D.H., *Four grams of glucose.* Am J Physiol Endocrinol Metab, 2009. **296**(1): p. E11-21.

83. Whiteman, E.L., H. Cho, and M.J. Birnbaum, *Role of Akt/protein kinase B in metabolism.* Trends Endocrinol Metab, 2002. **13**(10): p. 444-51.

84. Williamson, D.L., D.R. Bolster, S.R. Kimball, and L.S. Jefferson, *Time course changes in signaling pathways and protein synthesis in C2C12 myotubes following AMPK activation by AICAR.* Am J Physiol Endocrinol Metab, 2006. **291**(1): p. E80-9.

85. Wojtaszewski, J.F., A.B. Jakobsen, T. Ploug, and E.A. Richter, *Perfused rat hindlimb is suitable for skeletal muscle glucose transport measurements.* Am J Physiol, 1998. **274**(1 Pt 1): p. E184-91.

86. Wright, D.C., K.A. Hucker, J.O. Holloszy, and D.H. Han, *Ca2+ and AMPK both mediate stimulation of glucose transport by muscle contractions.* Diabetes, 2004. **53**(2): p. 330-5.

87. Youn, J.H., E.A. Gulve, and J.O. Holloszy, *Calcium stimulates glucose transport in skeletal muscle by a pathway independent of contraction.* Am J Physiol, 1991. **260**(3 Pt 1): p. C555-61.

88. Zhao, H., R. Hyde, and H.S. Hundal, Signalling mechanisms underlying the rapid and additive stimulation of NKCC activity by insulin and hypertonicity in rat L6 skeletal muscle cells. J Physiol, 2004. **560**(Pt 1): p. 123-36.

APPENDIX I: BREAKDOWN OF SIGMA MEDIA-199 (#4530)

Product Name	Medium 199, With Earle□s salts, L-glutamine and sodium bicarbonate, liquid, sterile-filtered, cell culture tested
Product Number	M4530
Product Brand	SIGMA

TEST	**SPECIFICATION**
Appearance (Turbidity)	Clear
Appearance (Form)	Solution
pH	7.0 - 7.6
Osmolality	280 - 310 mOs/kg
Cell Culture Testing - MTT	Pass
Cell Line	Cell Line - Cell Types
Key Element Conc - ICP	Pass
Amino Acid Analysis	Pass
Sterility	Pass
Endotoxin Level	<= 1 EU/ml
Glucose Concentration	0.9 - 1.1 g/l

Components		**M4530**
Inorganic Salts	[1X]	$g \bullet L^{-1}$
$CaCl_2 \cdot 2H_2O$		0.265
$Fe(NO_3)_3 \cdot 9H_2O$	0.00072	
$MgSO_4$ (anhyd)		0.9767
KCl		0.4
KH_2PO_4		--
Na·Acetate (anhyd)		0.05
$NaHCO_3$	2.2	
NaCl		6.8
Na_2HPO_4 (anhyd)		--
NaH_2PO_4 (anhyd)		0.122
Amino Acids		
DL-Alanine		0.05
L-Arginine·HCl		0.07
DL-Aspartic Acid		0.06
L-Cysteine·HCl·H_20		0.00011
L-Cystine·2HCl		0.026
DL-Glutamic Acid		0.1336
L-Glutamine		0.1
Glycine		0.05
L-Histidine·HCl·H_2O		0.02188
Hydroxy-L-Proline		0.01

DL-Isoleucine	0.04
DL-Leucine	0.12
L-Lysine·HCl	0.07
DL-Methionine	0.03
DL-Phenylalanine	0.05
L-Proline	0.04
DL-Serine	0.05
DL-Threonine	0.06
DL-Tryptophan	0.02
L-Tyrosine 2Na·2H_20	0.05766
DL-Valine	0.05
Vitamins	
Ascorbic Acid·Na	0.000056
D-Biotin	0.00001
Calciferol	0.0001
Choline Chloride	0.0005
Folic Acid	0.00001
Menadione (sodium bisulfite)	0.000016
myo-Inositol	0.00005
Niacinamide	0.000025
Nicotinic Acid	0.000025
p-Amino Benzoic Acid	0.00005
D-Pantothenic Acid·½Ca	0.00001
Pyridoxal·HCl	0.000025
Pydridoxine·HCl	0.000025
Retinol Acetate	0.00014
Riboflavin	0.00001
DL-α-Tocopherol Phosphate·Na	0.00001
Thiamine·HCl	0.00001
Other	
Adenine Sulfate	0.01
Adenosine Triphosphate·2Na	0.001
Adenosine Monophosphate·Na	0.000238
Cholesterol	0.0002
Deoxyribose	0.0005
Glucose	1.0
Glutathione (reduced)	0.00005
Guanine·HCl	0.0003
HEPES	--
Hypoxanthine	0.0003
Phenol Red·Na	0.0213
Tween 80	0.02
Ribose	0.0005
Thymine	0.0003
Uracil	0.0003
Xanthine·Na	0.000344

APPENDIX II: BREAKDOWN OF MANNITOL (#9546)

COPPER	<0.0005%
IRON	<0.0005%
LEAD	<0.001%
MAGNESIUM	<0.0005%
SODIUM	<0.005%
PHOSPHORUS	<0.0005%
ZINC	<0.0005%
POTASSIUM	<0.005%
PURITY	MINIMUM 98% BY GC OR HPLC
Product Name	D-Mannitol, BioXtra
Product Number	M9546
Product Brand	SIAL
CAS Number	69-65-8
Molecular Weight	182.17

TEST	**SPECIFICATION**
APPEARANCE	WHITE POWDER
SOLUBILITY	COMPLETE COLORLESS (1M IN WATER AT 20DEGC)
RESIDUE UPON IGNITION	<0.01%
AMMONIA CONTENT	<0.05%
INSOLUBLE MATTER	<0.01%
CHLORIDE (CL)	<0.05%
SULFATE (SO4)	<0.05%
ALUMINUM	<0.0005%
CALCIUM	<0.0005%

APPENDIX III: ATP/PCr ASSAY PROCEDURE

I. Reagents

0.5M PCA	21.5mL of 70% PCA
	Bring to 500mL with dH_2O; Store in 0-4°C for 1 month
2.3 M $KHCO_3$	2.3g $KHCO_3$
	Add 10.0mL dH_2O; Make Fresh Daily

II. Extraction Procedure

1. Freeze dry tissue (~12-24 hours to ensure all water is removed)
2. Store with dry rite in freezer until powdering
3. Tease out connective tissue and powder
4. Place in pre-weighed microcentrifuge tube and weight (3-5mg)
5. Place tubes in an ice-bucket (make sure tubes remain cold)
6. Add 600uL of pre-cooled 0.5M PCA
7. Extract for 10 minutes, vortexing several times
8. Centrifuge for 10 minutes at 15,000G (spinning helps remove some of the enzymes that can influence concentration)
9. Remove 540uL and place in freezer (-20°C) for 10 minutes
10. To the frozen supernatant add 135uL of 2.3M $KHCO_3$ and vortex until liquid (addition of $KHCO_3$ to a frozen supernatant prevents foaming over)
11. Centrifuge for 10 minutes, 0°C at 15,000G. Remove supernatant to assay metabolites.

III. Assay Procedure *(Note: run everything in triplicate)*

1. Prepare substrates (reagents 1-5 in section IV) without G-6-P-DH enzyme and bring to volume
2. Prepare ATP (Solid in -20) and PCr (aliquots found in -80) standards

3. Vortex each concentration before pipetting
    a. Fill the next 5 wells with 10.00µL of varying concentrations of ATP

4. Vortex each concentration before pipetting
    a. Fill the next 5 wells with 10.00µL of varying concentrations of PCr

5. Add G-6-P-DH enzyme to substrates and add 185µL of this buffer (pH 8.1) to each well

6. Incubate in a dark environment for 20 minutes, set up the fluorometer and read at 25 minutes

Part 2:

1. Mix 2.5µL of Hexokinase (HK) with 1mL of buffer. Mix by inversion.
2. Add 6µL of dilute HK to all of the wells
3. Incubate in a dark environment for 80 Minutes
4. Read the plate (excitation setting 340, emission setting 460)
5. R2-R1 = reflects [ATP] in extract

Part 3:

1. Mix ~1.5mg of phosphocreatine kinase and 5mg of ADP into 5mL of buffer. Mix by inversion
2. Add 6µL of dilute Creatine Kinase to all the wells
3. Place in a dark environment for 120 Minutes
4. Read the plate (excitation setting 340, emission setting 460)
5. R3-R2 = reflects [PCr] in extract

IV. Muscle Adenosine Triphosphate (ATP) and Phosphocreatine (PCr) Assay for Plate Reader Flourometer

P-Creatine + ADP ---CREATINE KINASE---> Creatine + ATP

ATP + Glucose ---HEXOKINASE---> ADP + Glucose-6-Phosphate

Glucose-6-Phosphate + NADP ---G-6-P-DH---> Glucanolactone + NADPH

Reagent	[Stock]	[Final]	Volume – 25mL	Volume – 50 mL	Volume – 100 mL
1. Tris (on shelf; pH 8.1) *stored in fridge*	1.00M	50mM	1.25mL	2.5mL	5.00mL
2. MgCl2 (on shelf; fresh) (.2033g/mL)	1.00M	1.0mM	25.00µL	50.00µL	100.00µL
3. D.T.T. (found in -20) *aliquots -80*	0.5M	0.5mM	25.00µL	50.00µL	100.00µL
4. Glucose (on shelf) *aliquots -80*	100.0 mM	100.0 µM	25.00µL	50.00µL	100.00µL
5. NADP (found in -20) *aliquots -80*	50.0 mM	50.0 µM	25.00µL	50.00µL	100.00µL
6. G-6-P-DH (liquid found in +4) (Sigma G-5760)	2660 U/mL	0.02 U/mL	1.00 µL	2.00 µL	4.00 µL
7. ATP (found in -20) (Sigma A-7699)	Solid – Refer to Section V				
8. Creatine Kinase (found in -20) (Sigma C-3755)	324 U/mL				

Note: Mix reagents 1-5 together. Bring to volume (23.649mL for 25mL) with distilled water and **adjust** pH to 8.1. Then add reagent 6. Mix by inversion with enzymes.

V. Standard Curves

ATP (Sigma A-7699)

Make fresh 5.51mg in 5 mL dH_2O

Concentration (mM)	Stock (µL)	dH_2O (µL)
0.05	25	975
0.1	50	950
0.2	100	900
0.3	150	850
0.4	200	800

Phosphocreatine (Sigma P-7936)

Stored in 5mM aliquots in the -80°C; (1.2755 g/L)

Concentration (mM)	Stock (µL)	dH_2O (µL)
0.1	20	980
0.2	40	960
0.4	80	920
0.8	160	840

APPENDIX IV: WESTERN BLOTTING

DAY 1: SAMPLE PREPARATION FOR WESTERN BLOTTING

HOMOGENIZATION

1. Set centrifuge to 4 degrees C.
2. Weigh wet muscle.
3. Add muscle and chilled homogenizing buffer to a chilled glass homogenizer (on ice) in the following proportions (try to keep muscle weights within this range):

Muscle Weights	*Homogenization Buffer*
<50 mg	700 μl
60 mg	850μl
70 mg	1000 μl
80 mg	1150 μl
90 mg	1300 μl
100 mg	1450 μl
110 mg	1600 μl
120 mg	1750 μl
130 mg	1900 μl

4. Add Protease Inhibitor cocktail (*Roche* 11836170001*;*1 tablet per 10mL of buffer)
5. Add Phosphatase Inhibitor cocktail (*Roche* 4906845001*;*1 tablet per 10mL)
6. 100 passes in chilled buffer using a glass pestle (on ice).
7. Rinse pestle with 100 μl of chilled homogenizer buffer (Solution # 1) into sample.
8. Decant into 1.5 ml eppendorf and centrifuge at 1200 x g for 10 min
9. Decant supernatant (SN1) and store in an eppendorf at -80 degress C. (typically, this supernatant will be the one with the highest protein concentration)
10. Resuspend pellet in 1 ml of chilled Triton X-100 buffer (Solution # 2; detergent, helps break up membranes; serial dilution) and vortex gently (also helps to break up the membranes).
11. Centrifuge at 1200 x g (1200 times the force of gravity) for 10 min @ 4°C.
12. Decant supernatant (SN2) and store in an eppendorf at -80 degrees C.
13. Resuspend pellet in 1 ml of chilled wash buffer (Solution #15) and store at -80 degrees C. Store this as (Pellet).

PROTEIN ASSAY

It is very important that this be done accurately, as it is imperative that equal amounts of protein are loaded in each lane for the electrophoresis.

1. A standard curve using bovine serum albumin (BSA) (Boehringer-Mannheim; 735-708; stored in FREEZER) is run with each new microtitre plate. Each point on the calibration curve is run in triplicate.
2. Start with a 1 mg/ml BSA protein standard (Pre-made in the -20 Freezer). Label 7 eppendorf tubes: 0.5, 0.4, 0.3, 0.2, 0.1, 0.05, 0. Following the chart below, dilute the 1

mg/ml stock solution to yield desired protein concentrations. Final volume = 50ul (require 3 x 10ul = 30ul, but make more to be safe)

3. Calibration curve protein concentrations:

Desired Protein Concentration (mg/ml)	*Volume of 1 mg/ml BSA Standard (ul)*	*Volume of ddH2O (ul)*
0.5	25	25
0.4	20	30
0.3	15	35
0.2	10	40
0.1	5	45
0.05	2.5	47.5
0	0	50

4. Dilute each of the muscle samples 10x as well; 90 μl ddH2O and 10 μl sample.
5. VORTEX and pipette into the wells of the microtitre plates 10 μl of the newly diluted BSA in triplicate to establish a standard curve.
6. Vortex and pipette into the wells of the microtitre plates 10 μl of diluted sample in triplicate.
7. Using a multi-channel pipette add 200 μl of diluted reagent (1:4 dilution with Bio-Rad Protein Assay Dye Reagent Concentrate: DH_20) into each well.

USING THE FLUOROMETER

8. Open the 'KC4' software.
9. Click on the 'Wizard' icon and select 'Reading Parameters'.
10. Click '**End Point'** assay, make sure '**Absorbance'** is also checked.
11. **Wavelength** should be set to 595 nm, **Intensity** set to 3, and **Duration** set to 5.
12. Click OK.
13. Select the "Read"
14. Once the plate has been read, click on '**Data'** and choose **Export**.
15. In the 'Plates' drop down menu, choose 595 nm.
16. Copy and Paste to Excel and use the "Text to Column" (by semi colon) function.

Article I.

DAY 2: GEL ELECTROPHORESIS AND MEMBRANE TRANSFER

CAST GEL

Note: Gels can be made and stored in the refrigerator (2-8° C) one day prior to gel electrophoresis and membrane transfer. If gels are to be made in advance, follow the procedure below until step 3. After completing step 3 wrap the gel in saran wrap (leaving the comb inserted into the gel), and store in the refrigerator.

Use ProtoGel Buffer System; otherwise an alternative method is given.

To make up four 1mm thick mini-gels:

	7.5% Separating Gel	*10% Separating Gel*	*12% Separating Gel*	*4% Stacking Gel*
ddH_2O	9.7ml	8.02ml	6.66 ml	6.1ml
Separating buffer (Resolving Buffer)	5.0ml	5.0ml	5.0 ml	-
Stacking Buffer	-	-	-	2.5ml
ProtoGel (30% Acrylamide/0.8% Bis)	5.0ml	6.66ml	8.02 ml	1.33 ml
10% AP Solution** (Solution #9)	200µl	200µl	200µl	100µl
Temed***	20µl	20µl	20µl	20µl

(i) **Do NOT add AP and Temed until immediately before casting the gel.
***Do this step in the fumehood.
Essentially, as acrylamide increases, the pore size decreases and vice versa. Large pores are used for large proteins and vice versa.
To make a gel of X percentage, follow this formula:

% Gel = (X mL of 30% Acrylamide/0.8% Bis/Total Volume) * 0.3*100
E.g. % Gel = (10 mL of 30% Acrylamide/0.8% Bis/Total Volume) * 0.3*100
= 10/20*0.3*100
= 15%

The total volume should remain constant at 20 ml. If you are adding more 30% Acrylamide/0.8% Bis, take this volume from the dH20.

Molecular Weight Range for % Separating Gel				
>250 kDa = 4-5% Gel	250-120 kDa = 7.5% gel	120-40 kDa = 10% gel	40-15 kda = 13% gel	<20 kda = 15% gel

Clean 1.0 mm spaced plates with 70% ethanol. Once set up, pipette in dH_20 between the plates and let stand 5-10 min. If the water level drops, there is a leak in the bottom seal, therefore set up apparati again and re-check with water. When the water level is stable after 5-10 min, then drain it, wipe edges with Kim-Wipe, and go to step 2.

1. Pour in your separating gel (see above Table for making this solution) using a Pasteur pipette until the gel is ~1cm from the bottom of where the wells would be. It is **ESSENTIAL** to have approx. 0.5-1 cm of stacking gel on top of the separating gel so that the proteins can separate before moving into the separating gel.
2. Pour slowly (from the middle of the plate) to prevent bubbles from forming, and immediately overlay with dH_20 or methanol. Add the dH_20 or methanol slowly and evenly. Allow the gel to polymerize for 45min at RT. The methanol will ensure that the gel polymerizes evenly and that there are no bubbles.

CAST STACKING GEL (1 HOUR)

3. Drain the methanol or dH_20 from top of gel, and dry edges with Kim wipe. Place the comb half way into the plates. Pour in stacking gel (see above table for making this solution) until the top of the short plate, and then push the comb in fully. Allow gel to polymerize for 30 min to an hour at RT.

PREPARE SAMPLES WHILE STACKING GEL IS POLYMERIZING

To ensure consistency between western blots, it is essential to minimize the number of freeze-thaw cycles. Repeated freeze-thaw cycles will affect the quality of the homogenate, thus making it very difficult to keep amount of protein loaded consistent. **Refer to the Excel Spreadsheet on Computer.**

4. Now we are going to prepare samples to load in the wells. If we want: X μg of muscle protein/lane (as an example, we want 40 ug)
5. Volume of homogenate (μl) = 40 μg / homogenate concentration (μg/μl)
6. Volume per lane on a 10 lane, 0.75 mm thick gel = 25μl (but we will make 45 ul).
7. Ratio of *(homogenate + dilution buffer) : Sample Buffer* is ALWAYS *2:1* or *30μl : 15μl*.
8. Volume of dilution buffer = 30ul – volume of muscle homogenate.
9. Follow the company specific preparation directions for the molecular weight standard. (BioRad Precision Plus Kaleidoscope MW Marker works well).
10. Vortex gently. Poke a hole in the top of each eppendorf with a needle and heat your samples for 6 min at 95°C. Cool on crushed ice for at least 5 min.
11. Flash-spin down the sides in microcentrifuge (20 seconds on high revolution).

Ex:Total [protien]	Amount for 40 ug	Dilution buffer	Sample buffer
(a) 1.89 ug/ul	40ug / 1.89ug/ml = 21.16 ul	30ul – 21.16ul = 8.84 ul	15 ul
(b) 2.39 ug/ul	40ug / 2.39 ug/ul = 16.74 ul	30ul – 16.74 ul = 13.26 ul	15 ul

GEL ELECTROPHORESIS (1 HR AT 200V OR 3 HRS AT 70V)

12. CAREFULLY remove the comb and clean out each well using thin pieces of filter paper.
13. Slide the gel cassettes into electrode assembly and buffer chamber with the short plate facing IN, then add running buffer (working solution) to the inner chamber until it overflows. If you are only using one gel, be sure to use the buffer dam.
14. Load appropriate volume of your sample using specialized gel-loading tips.
15. Add 5ul of Kaleidescope (Bio-Rad, 161-0375)
16. Top up both chambers with 1 x Tris-Glycine Running Buffer (the working solution – see Solution # 10). Connect assembly to power supply and run gels at 120V until fully migrated (~90mins). Stop the current when the blue band reaches the bottom of the gel.
17. While the proteins are migrating, make fresh TBST and Transfer Buffer.

GEL-MEMBRANE TRANSFER

18. Prior to use, the PVFD membrane (Bio-Rad, #162-0184) has to be immersed in methanol for 10 seconds (to open the pores). Where gloves and handle membrane with tweezers.
19. Place filter papers (extra thick blot paper, 7 x 8.4 cm, BioRad Cat #: 1703966; ~6 per gel), the gel, filter pads (2 per gel) and membrane in Transfer Buffer (Solution #12) and then allowed to equilibrate in transfer buffer for ~10-15 min. (use Tupperware containers).
20. Assembly of sandwich plates:

    White – Filter Pad – 3 Filter Papers – Membrane – Gel – 3 Filter Papers – Filter Pad - Black (Back)
21. Roll out each layer with a glass test tube to eliminate air bubbles
22. Close sandwich plates and insert into transfer apparatus.

23. Place the safety cover on the unit, plug in and run at 100 volts for 90 minutes (limit to 5.5 mamps/cm^2 gel).
24. Once transfer is complete, discard filter papers and set filter pads aside.
25. Cut membrane in the shape of the gel, using a sharp knife. Remember to make an extra cut on the corner for the top kaleidoscope corner.

MEMBRANE BLOCKING (1 HOUR or more)

***Blocking is done to prevent non-specific antibody binding to other proteins.*

26. Once transfer is complete, carefully remove membranes from the sandwich and place FACE-UP in square petri dishes. Wash once for 10 minutes in TBS with gentle agitation.
27. Block membrane with Solution #14 (milk) for 1 hour at room temperature with gentle agitation. Use 10mL of blocking solution.
28. Wash 5x5min with 10mL of TBST

INCUBATE MEMBRANE WITH PRIMARY ANTIBODY OVERNIGHT

29. Dilute the primary antibody in a recommended/optimized ratio of Ab : blocking solution (see Solution #14, milk).
30. Apply this primary antibody solution and incubate 12-24 hours with agitation in fridge.

DAY 3: EXPOSE/DEVELOP FILM AND BAND DENSITY DETERMINATION

INCUBATE MEMBRANE WITH SECONDARY ANTIBODY (1 hour)

31. Make fresh TBST.
32. Pour our excess solution. Wash with fresh TBST. Wash 5 times for 5 minutes each in TBST with gentle agitation.
33. Use enough (10-15mL) TBST to cover the membrane each time
34. For AMPK, add 7.5 ul of 2°Ab into 15 ml of milk (2°Ab: AMPK Cell Signaling Tech. # ____). Incubate for 1 hr at RT with agitation.

INCUBATE MEMBRANE WITH TAGS (~15 min)

35. Wash each membrane 5 times each (5x5mins), with enough (fresh) TBST to cover with gentle agitation. Blot the membranes dry and place into a clean square petri dish for development.

Alpha Innotech: FluoroChem 5500 Gel Imaging System

36. For the Gel Dock, use Chemi Glow West Substrate (Fisher, Cat. # CGW-8000).
37. Dry membrane; use tweezers and touch a corner to kim wipe and empty the petri dish
38. Take 1mL from each bottle and combine in the petri dish/membrane
39. For the 1st membrane you must manually "agitate" for 5 minutes
40. For the 2nd membrane reuse the 2mL from the 1st membrane and add an additional 2mL of Chemi Glow
41. For the 3rd, 4th etc membrane reuse the 4mL from the first two membranes
42. Incubate for 5 minutes with agitation at room temperature.
43. Place the Petri dish in the Gel Dock and run the 'Auto Expose' function. Once the required exposure time has been found, you can now manually adjust it until your bands become saturated. Expose until the point where your bandings are not over-saturated. (This can be accomplished using the 'Saturation' icon at the top of the screen)

SOLUTIONS

1. Homogenization Buffer 250 mM sucrose = 21.4 g 100 mM KCl = 1.865 g 5 mM EDTA = 0.4695 g (Dihydrate form) Add to 225 ml dH2O, fix pH to 6.8, top up to 250 ml dH2O and mix well. Store at 4°C.	**2. Triton X-100 Buffer** 175 mM KCl = 1.305 g 0.5% Triton X-100 = 0.5 ml Add to 90 ml dH2O, pH to 6.8, top up to 100 ml dH2O and mix well. Store at 4°C.
3. Sample Buffer (SDS Reducing Buffer): 2.05 dH_2O 1.25ml 1.5M Tris-HCl, pH 6.8 3 ml glycerol 2.0ml of 30% SDS (w/v) (3g SDS in 10 mL H20) 1.5ml Beta-mercaptoethanol 0.2 ml of 0.5% w/v Bromphenol Blue Mix well; store at 4°C.	**4. Dilution Buffer:** 2.796g (150mM) KCl 0.6055g (20mM) Tris Base Dilute in 250ml of ddH_2O; adjust pH to 7.0.
5. Separating Buffer: 27.23 g Tris-base (Boehringer Manneheim, #604-205) 80 ml dH_20 Adjust pH to 8.8 with HCl. Fill to 150 ml with dH_20 and store at 4°C.	**6. Stacking Buffer:** 6 g Tris base (Boehringer Manneheim, #604-205) 60 ml dH_20 Adjust to pH 6.8 with HCl and fill to 100 ml with dH_20.
7. 30% Acrylamide/8% Bis: 87.6 g acrylamide (Gibco BRL, #15512-031) 2.4 g N'N' bis-methylene acrylamide (BioShop, #BIS-001) Fill to 300 ml with dH_20 and store in the dark at 4°C (i.e. wrap in aluminum foil). Re-make fresh each month.	**8. 10% Sodium Dodecyl Sulfate:** 10 g sodium lauryl sulfate (SDS) (BDH, #B30175) Add 10 g of SDS and fill to 100 ml with dH_20. Store at room temperature.
9. Ammonium Persulfate: 0.06 g ammonium persulfate (APS) (Sigma, #A-3578) Weigh into an Eppendorf. Add 600 μl of dH_20. Make fresh daily.	**10. 10 x Tris-GlycineRunning Buffer:** 30g Tris-base (Boehringer Manneheim, #604-205) 144 g glycine (BDH, #B10119) 10 g SDS (BDH, #B30175) Add 1L dH_20. Do not adjust pH.
16. Coomaisse Blue Stain for Gels and Membranes for Protein Detection 40 ml Methanol 10 ml Acetic Acid 0.25 g Coomassie Blue 50 ml dH2O	**12. Transfer Buffer (1000ml/buffer chamber):** Towban Buffer: 3.03 g Tris Base 14.4 g glycine 200 ml methanol 800 ml dH20
13. 10 x TBST: 24.28g Tris Base 80.06g NaCl 1 L dH20 pH 7.5	**14. 5% Blocking Solution:** *BSA:* Dissolve 7.5 g skim BSA (Sigma, A3059) in 150 mL of TBST *Milk:* Dissolve 7.5 g skim milk (from grocery store) in 150 ml TBST (5g/100mL)

APPENDIX V: SPECIFIC WESTERN BLOT PROTOCOLS

Protein	**MW** (kDa)	**%Gel**	**Membrane**	**SDS-Page**	**Transfer**	**Block**	**Primary**	**Secondary**	**Antibody Details**
pAMPK	63	10	NC	90 mins @ 120V	90 mins @ 100V	5% Milk	1:1000	1:10,000	Cell Signaling #4188
pPKCα	82	8	PVDF	90 mins @ 120V	90 mins @ 100V	2.5%BSA	1:500	1:3000	Millipore #06-822
pERK2	44	10	PVDF	90 mins @ 120V	90 mins @ 100V	5%BSA	1:2000	1:10,000	Cell Signaling #4370
pAkt Thr308	60	10	PVDF	90 mins @ 120V	90 mins @ 100V	5%BSA	1:1000	1:10,000	Cell Signaling #2965
pAS160	160	8	PVDF	90 mins @ 120V	120 mins @ 90V	7.5%BSA (3hrs)	1:1000	1:1000	Invitrogen/Biosource #44-1071G